

## Cosmos 462 (1971-106A): Orbit Determination and Analysis

Doreen M. C. Walker

*Phil. Trans. R. Soc. Lond. A* 1979 **292**, 473-512

doi: 10.1098/rsta.1979.0070

### Email alerting service

Receive free email alerts when new articles cite this article - sign up in the box at the top right-hand corner of the article or click [here](#)

To subscribe to *Phil. Trans. R. Soc. Lond. A* go to: <http://rsta.royalsocietypublishing.org/subscriptions>

# COSMOS 462 (1971–106A): ORBIT DETERMINATION AND ANALYSIS

BY DOREEN M. C. WALKER

*Royal Aircraft Establishment, Farnborough, Hampshire, U.K.*

*(Communicated by D. G. King-Hele, F.R.S. – Received 24 November 1978)*

## CONTENTS

	PAGE
1. INTRODUCTION	474
2. THE OBSERVATIONS	475
3. THE ORBITS OBTAINED AND THE OBSERVATIONAL ACCURACY	475
3.1. The orbits	475
3.2. Accuracy of the observations	479
4. ORBITS FOR THE 15 DAYS BEFORE DECAY	479
5. ANALYSIS OF VARIATION IN INCLINATION AND ECCENTRICITY AT RESONANCE	481
5.1. Theoretical equations for $\beta : \alpha$ resonance	481
5.2. Fourteenth-order (14:1) resonance	483
5.2.1. Equations for 14:1 resonance	483
5.2.2. Analysis of inclination, $i$	484
5.2.3. Analysis of eccentricity, $e$	485
5.2.4. Inclination and eccentricity fitted simultaneously	487
5.3. 29:2 resonance	487
5.3.1. Equations for 29:2 resonance	488
5.3.2. Analysis of inclination, $i$	489
5.3.3. Analysis of eccentricity, $e$	490
5.4. Fifteenth-order (15:1) resonance	491
5.4.1. Equations for 15:1 resonance	491
5.4.2. Analysis of inclination, $i$	492
5.4.3. Analysis of eccentricity, $e$	493
5.4.4. Inclination and eccentricity fitted simultaneously	494
6. ATMOSPHERIC ROTATION	495
6.1. Introduction	495
6.2. Theory	495
6.3. Fitting of theoretical curves to the inclination	497
6.4. Results	499
7. DENSITY SCALE HEIGHT	500
7.1. Introduction	500
7.2. Method	501
7.3. Discussion of results	502

	PAGE
8. CONCLUSIONS	503
REFERENCES	505
TABLES 1, 2 AND 4	506

Cosmos 462 (1971–106A) was launched on 3 December 1971 into an orbit inclined at  $65.75^\circ$  to the equator, with a perigee height of 230 km and apogee height of 1800 km. The satellite remained in orbit for 40 months and decayed on 4 April 1975. Orbital parameters have been determined at 85 epochs by using the R.A.E. orbit refinement program PROP, with 6635 radar and optical observations, including 197 from the Hewitt cameras. The average standard deviation in eccentricity and inclination corresponded to a positional accuracy of about 100 m. In addition, orbits of similar accuracy were determined daily for the last 15 days of the life, from 2000 NORAD observations.

During its slow decay, the orbit passed through 14 : 1, 29 : 2 and 15 : 1 resonances with the Earth's gravitational field. The variations in inclination and eccentricity at these resonances have been analysed in detail to evaluate lumped geopotential harmonic coefficients of order 14, 29 and 15.

The variation of inclination between resonances has been analysed to obtain four values of the average atmospheric rotation rate  $A$  at heights of 200–250 km in 1972–5. The values of  $A$  show a seasonal dependence, being greater in winter than in summer, and the average rotation rate is lower than in the 1960s, being near 1.0 rev/day. Analysis of the inclination in the last 15 days of the satellite's life indicates a weak west-to-east wind at high latitude ( $54$ – $62^\circ$  N).

The variation of perigee height has been analysed to obtain 24 values of density scale height  $H$ , including eight in the last 15 days. Comparison with values from CIRA 1972 shows a bias difference of only 1% and r.m.s. difference of 10%, so CIRA 1972 provides a good approximation to the values of  $H$  in 1972–5.

## 1. INTRODUCTION

Cosmos 462 entered orbit on 3 December 1971 and was one of a pair of satellites launched by the U.S.S.R. to test high-speed interception (Sheldon 1976; Freedman 1977; Perry 1977). Cosmos 462 was the hunter satellite and exploded after passing the target satellite, Cosmos 459. This explosion occurred 3.5 h after launch and the largest piece of the satellite remaining in orbit was designated 1971–106A.

After this experiment, 1971–106A had an orbital period of about 105 min, perigee height 230 km, apogee height 1800 km and inclination,  $i$ ,  $65.7^\circ$ ; the satellite remained in orbit for 40 months, without further disturbance and decayed naturally on 1975 April 4.90 (Pilkington *et al.* 1979).

Early in its lifetime, 1971–106A was selected for high-priority observing by the British optical and radar tracking stations, including the Hewitt cameras at Malvern and Edinburgh; 1971–106A was in an orbit which would be useful for determining the atmospheric rotational speed from the decrease in orbital inclination, and air density at heights near 200 km could be evaluated from its decay rate.

The orbit of 1971–106A has been determined from all available observations with the aid of the R.A.E. orbit refinement program PROP (Gooding & Tayler 1968), in the PROP 6 version (Gooding 1974), at 85 epochs during its 40 month life. In addition 15 daily orbits at the end of the life were determined from NORAD observations. This paper describes the orbit determinations, and the

analyses of variations in the orbital parameters. The changes in inclination and eccentricity at 14:1, 29:2 and 15:1 resonances have been analysed to determine lumped geopotential coefficients of order 14, 29 and 15. (There was no detectable perturbation at 31:2 resonance.) The values of inclination between the resonances have been analysed to determine the atmospheric rotation rate at heights near 200 km. The accurate values of perigee height obtained, which have already been used in evaluating the air density (Walker 1978*a*), have been analysed to determine the atmospheric density scale height. The residuals of the observations have been used to assess the accuracy of each observing station.

## 2. THE OBSERVATIONS

The orbit of 1971–106A has been determined at 85 epochs from 6635 observations. A breakdown of the number and type of observations used on each of the 85 runs is given in table 1 on page 506.

The observations can be divided into six groups (see table 1), the most accurate being those from the Hewitt cameras at Malvern (M) and Edinburgh (E). These observations, which were available on 43 transits, 29 from Malvern and 14 from Edinburgh, usually have an accuracy of 2" in direction and 1 ms in time.

The observations in the second group, made by the kinetheodolite at the South African Astronomical Observatory, have a directional accuracy of 1'. These observations are very valuable because they can greatly improve the orbital accuracy, especially the values of eccentricity, as they are made in the southern hemisphere, whereas northern-hemisphere observations are predominant.

The third group consists of visual observations made by volunteer observers reporting to the Radio and Space Research Station (now Appleton Laboratory), Slough, and to the Moonwatch Division of the Smithsonian Astrophysical Observatory. These visual observations usually have directional accuracies between 1' and 4'. This group accounted for about 20% of the total number of observations available.

The fourth group of observations are those made by British radar stations. About 80 observations were made by the radar tracker at R.R.E., Malvern, and the rest, around 2250, by the radar trackers at R.A.F., Fylingdales.

The fifth group consists of U.S. Navy observations, supplied by the U.S. Naval Research Laboratory. Some 2550 observations were available with a topocentric accuracy of about 2'. The final group of 120 observations comes from the theodolite at Jokioinen, Finland, with accuracy of about 5'.

## 3. THE ORBITS OBTAINED AND THE OBSERVATIONAL ACCURACY

### 3.1. *The orbits*

Orbits were determined at 85 epochs fairly evenly spaced over the satellite's life, and the orbital elements at each epoch are listed in table 2 (on pp. 508–511) with the standard deviations below each value. The epoch for each orbit is at 00 h on the day indicated. In the PROP6 model (Gooding 1974) the mean anomaly  $M$  is fitted by a polynomial of the form

$$M = M_0 + M_1 t + M_2 t^2 + M_3 t^3 + M_4 t^4 + M_5 t^5, \quad (1)$$

where  $t$  is the time measured from epoch and the number of  $M$ -coefficients used depends on the drag. For a high-drag orbit like that of 1971–106A, the number of coefficients to be used is found by trial and error. Best results were obtained by using  $M_0$  to  $M_5$ , the full complement of coefficients allowed in the PROP model, for 32 of the 85 orbits; 33 orbits required  $M_0$  to  $M_4$ ; 16 orbits  $M_0$  to  $M_3$  and the remaining 4 needed only coefficients  $M_0$  to  $M_2$ .

The orbits all fit the observations in a satisfactory manner, with  $\epsilon$ , the parameter indicating the measure of fit, ranging between 0.99 and 0.30, where  $e^2$  is the sum of the squares of the weighted residuals divided by the number of degrees of freedom; and the weighted residual is defined as the value (of right ascension or declination) given by the orbit, minus the value given by the observation, divided by the *a priori* error assigned to the observation. No particular difficulty in fitting was experienced at the times of magnetic storms, when the drag is liable to vary irregularly. For example, the orbit at the time of the major solar disturbance in early August 1972 fitted well.

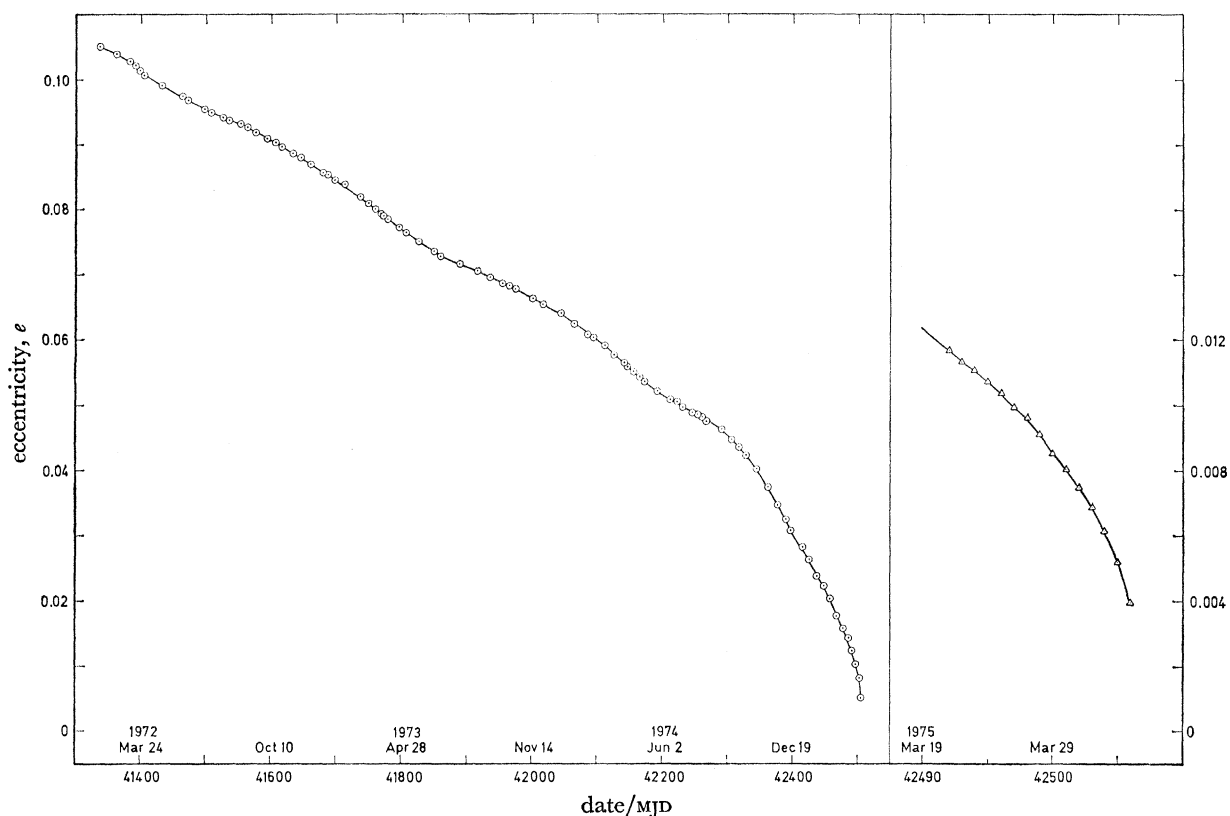


FIGURE 1. Variation of eccentricity,  $e$ .  $\odot$ , from orbits of table 2;  $\triangle$ , from table 4.

Hewitt camera observations were available for inclusion in 24 of the orbits determined (see tables 1 and 2). For these 24 orbits the standard deviation (s.d.) in eccentricity ranged from 0.000002 to 0.000029 with an average of 0.000012, corresponding to about 80 m in perigee or apogee height. The standard deviations in inclination varied from  $0.0001^\circ$  to  $0.0011^\circ$  giving an average s.d. of  $0.0006^\circ$ , also equivalent to about 80 m in distance. The other 61 orbits, those without Hewitt camera observations, had standard deviations in inclination varying from  $0.0007^\circ$  to  $0.0030^\circ$  with an average of  $0.0014^\circ$ , equivalent to some 170 m in distance, more than double the average s.d. of the orbits with Hewitt camera observations. The improvement in accuracy for

eccentricity is less significant, being about 15%. The same increase in accuracy for eccentricity is achieved on those orbits by using the Cape kinetheodolite observations. This confirms the opinion already expressed that, while the Hewitt camera observations greatly improve the accuracy of the orbital inclination (and the other orbital parameters to a lesser degree), the southern-hemisphere observations have a great influence in defining the shape of the orbit, as shown by the increased accuracy in eccentricity.

Figure 1 shows the values of eccentricity, from table 2: the gradual decrease due to drag is the dominant feature; for most satellites the oscillation due to odd zonal harmonics is usually also important, but it is so small as to be imperceptible for 1971–106A, because the inclination ( $65.7^\circ$ ) is close to the value ( $66.1^\circ$ ) where the effect of the third zonal harmonic is cancelled by the effects of the fifth and higher harmonics (see King-Hele & Cook 1974). The maxima and minima in slope of the curve in figure 1 coincide with the minima and maxima in the variation of the satellite's perigee height, which occur when the perigee is at the equator or at maximum latitude. Figure 4 of Walker (1978*a*) shows that perigee height has maxima at MJD 41 575, 41 920 and 42 240, and minima at MJD 41 410, 41 760, 42 105 and 42 420. (The triangles in figure 1 indicate values from the daily orbits for the last 15 days of the life; MJD is modified Julian day.)

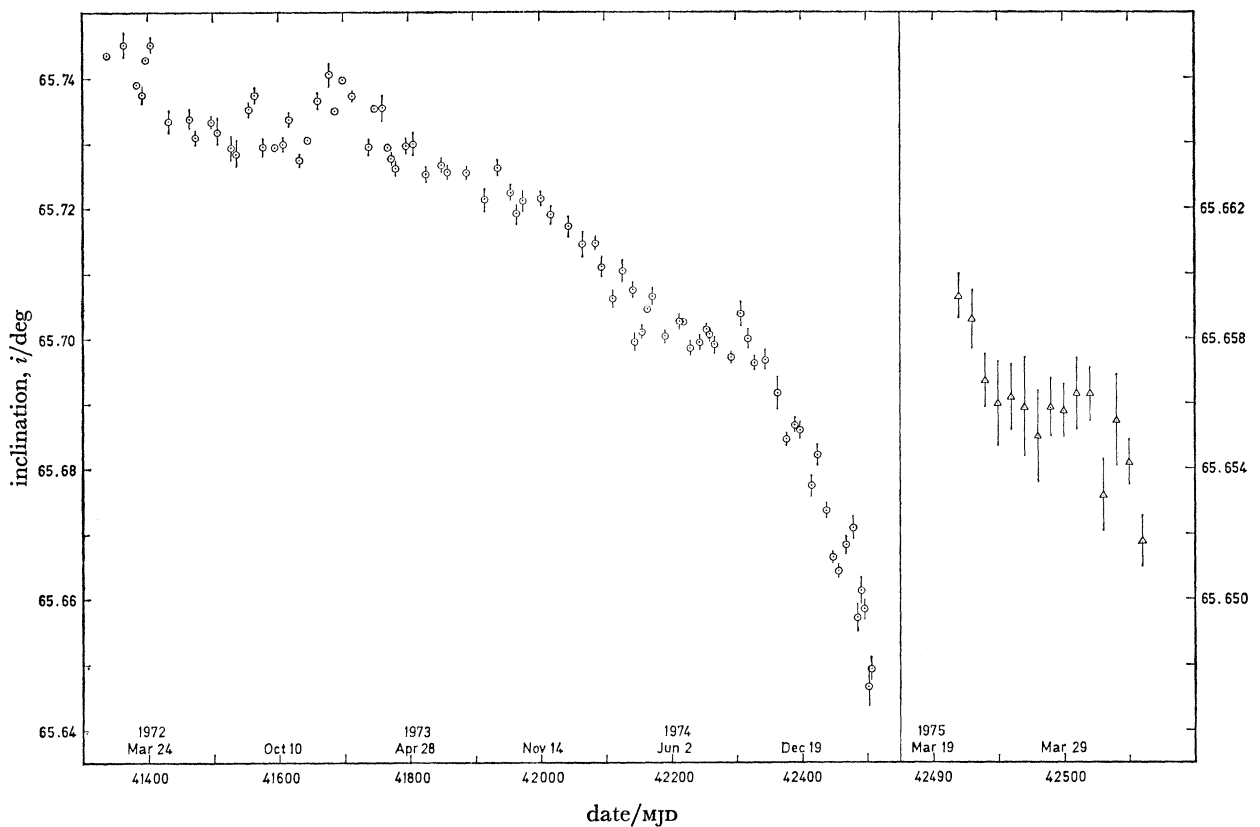


FIGURE 2. Variation of inclination,  $i$ ,  $\odot$ , from orbits of table 2;  $\triangle$ , from table 4.

Figure 2 shows the values of inclination,  $i$ , from table 2 (and table 4). These values of inclination are irregular, and before any meaningful conclusions can be drawn from the variation of inclination, the values must be cleared of all perturbations (see §§5 and 6). However, the

perturbing effects of the 14th- and 15th-order resonances are discernible in the observational values, at dates centred on MJD 41 659 and 42 302 respectively.

The accuracy of other orbital parameters is much as expected. Most of the values of right ascension of the node,  $\Omega$ , have standard deviations of  $0.001^\circ$  or  $0.002^\circ$ , generally slightly higher than the s.d. in the inclination. In the first half of the life, the argument of perigee,  $\omega$ , is accurate to  $0.01^\circ$ , but as usual the s.d. tends to vary as  $e^{-1}$  and increases considerably towards the end of the life as  $e \rightarrow 0$ .

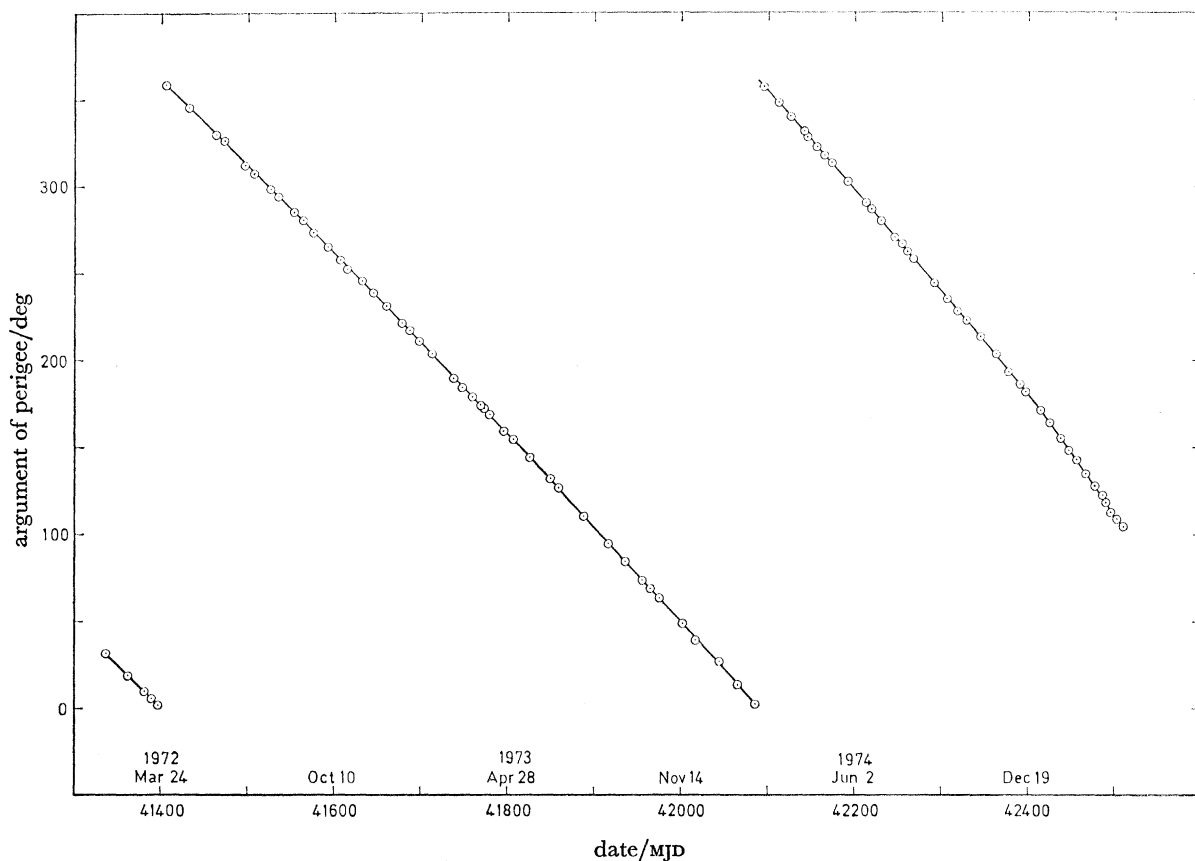


FIGURE 3. Variation of argument of perigee,  $\omega$ .

The variation of  $\omega$  for 1971-106A is much slower than for most satellites, because the inclination is quite close to the critical value of  $63.4^\circ$ , for which  $\dot{\omega} = 0$ . Figure 3 shows the values of  $\omega$  from table 2: the argument of perigee decreases by about  $\frac{1}{2}^\circ$  per day, and perigee does not quite complete 2 revolutions during the 40 months of the satellite's life.

Nearly all the values of  $M_1$  are accurate to better than 1 part in  $10^6$ , and consequently nearly all the values of semi major axis,  $a$ , have standard deviations of between 1 and 3 m.

The values of  $M_2$ , which provide a direct measure of the air drag (Walker 1978*a*), are mostly accurate to better than  $\frac{1}{2}\%$ : they are plotted in figure 4 and have been fully utilized and discussed in Walker (1978*a*).

### 3.2. Accuracy of the observations

The orbit refinement program proceeds by rejecting observations which do not fit well (weighted residuals  $> 3\epsilon$ ): a total of 5449 observations out of the original 6635 were accepted in the final orbits.

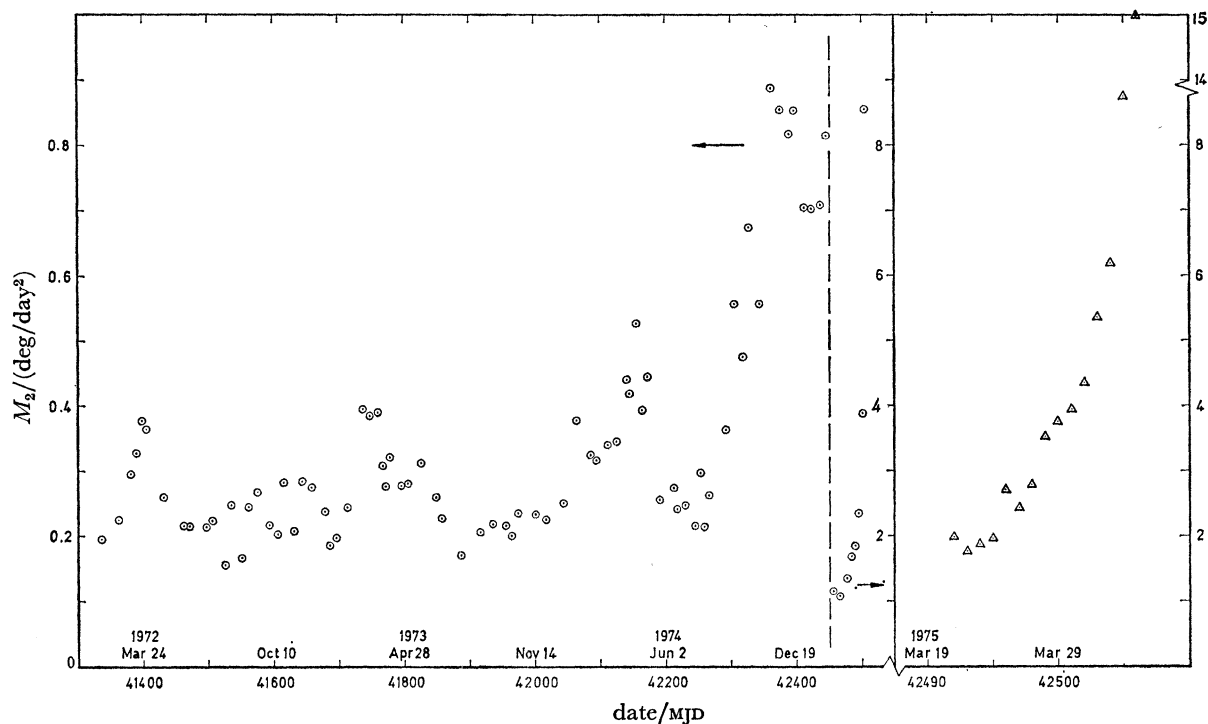


FIGURE 4. Variation of  $M_2$ .  $\odot$ , from orbits of table 2;  $\Delta$ , from table 4.

The residuals of the observations have been obtained by using the ORES computer program (Scott 1969) and sent to the observers. The accuracies of selected observing stations, with five or more observations accepted in the orbit determination, are listed in table 3, along with the number of accepted observations. The U.S. Navy observations from station 29 are geocentric, and if they were given in the same form as the other (topocentric) observations, their angular r.m.s. residuals would increase by a factor of about 5. The total r.m.s. residuals in table 3 are much as expected: 0.04' for the Hewitt cameras, 1.3' for the Cape kinetheodolite, and from 2.0' upwards for the visual observers and theodolites.

### 4. ORBITS FOR THE 15 DAYS BEFORE DECAY

After the orbital determinations described in §3 were completed, a further 2000 observations were provided by the assigned and contributing sensors of the North American Air Defense Command (NORAD) Space Detection and Tracking Systems (SPADATS) for the last 15 days before decay. With the aid of these observations it has been possible to determine orbits at the end of the satellite's life more accurately and at closer intervals than has been possible in the past.

Fifteen further orbits were determined at daily intervals from 1975 March 21.0 by using these NORAD observations together with other observations previously used in orbits 83–85 of table 2.



TABLE 3. RESIDUALS FOR OBSERVING STATIONS WITH MORE THAN FIVE OBSERVATIONS ACCEPTED IN THE ORBIT DETERMINATION

station	number of observations accepted	r.m.s. residuals			
		range km	minutes of arc		
			r.a.	dec.	total
1 U.S. Navy	245		1.9	2.0	2.8
2 U.S. Navy	104		1.9	2.0	2.8
3 U.S. Navy	103		1.5	1.5	2.1
4 U.S. Navy	110		1.6	1.5	2.2
5 U.S. Navy	154		1.7	1.6	2.3
6 U.S. Navy	185		1.8	1.8	2.5
29 U.S. Navy	1275	0.6	0.3	0.4	
81 } Londerzeel	7		1.5	1.3	2.0
2594 }					
414 Capetown	89		3.2	3.4	4.7
725 Bucharest	7		4.0	6.2	7.4
1114 Miskolc	10		3.3	2.9	4.4
1963 Jokioinen	109		3.7	3.0	4.7
2265 Farnham	35		2.1	2.0	2.9
2303 Malvern	106		0.03	0.03	0.04
Hewitt camera					
2304 Malvern radar	78	1.3	2.0	2.5	
2406 Dublin	7		2.2	2.7	3.5
2414 Bournemouth	168		4.0	4.2	5.8
2419 Tremadoc	35		2.6	2.7	3.7
2420 Willowbrae	227		2.2	2.2	3.1
2421 Malvern 4	159		1.7	1.7	2.4
2430 Stevenage 4	14		1.8	1.5	2.3
2437 Warrington	7		3.9	4.7	6.1
2502 Sudbury	6		6.0	5.8	8.3
2513 Colchester	7		4.9	10.1	11.2
2528 Aldershot	7		1.7	1.6	2.3
2534 Edinburgh	51		0.03	0.02	0.04
Hewitt camera					
2539 Dymchurch	7		1.3	1.8	2.3
2550 Masirah	22		1.6	2.2	2.7
2577 Cape	89		0.9	1.0	1.3
kinetheodolite					
2596 Akrotiri	40		3.1	3.9	5.0
4126 Groningen	13		2.6	2.3	3.5
4130 Denekamp	8		3.7	4.4	5.7
8597 Adelaide	16		2.2	3.1	3.8

The orbital elements are listed in table 4 (on p. 512), with the standard deviations below each value. As before, the epoch for each orbit is at 00 h on the day indicated. In 11 of these 15 orbits, only the coefficients  $M_0$ ,  $M_1$  and  $M_2$  were required in the polynomial for mean anomaly, equation (1). This is unusual, because the full set of coefficients is generally needed near decay (as in table 2): here, however, the observations for each orbit extend over no more than 24 h, so that  $t \leq 0.5$  and terms in  $t^3$ ,  $t^4$  and  $t^5$  have much less effect than when  $t > 1$  as for the orbits of table 2. For example, if the set of coefficients in orbit 84 of table 2 were correct, the value of  $M_4 t^4 (= 0.05t^4)$  would be  $< 0.003^\circ$  for  $t < 0.5$ . So the term would not be significant for the one-day orbit, and  $M_4$  would not be needed. The values of  $e$ ,  $i$  and  $M_2$  from table 4 have been added at the right of figures 1, 2 and 4 respectively.

The last three orbits in table 2 (orbits 83, 84 and 85) are virtually independent of the corresponding orbits in table 4 (orbits E, J and N), because the latter orbits include only a few of the original observations, which are greatly outweighed by the large number of NORAD observations. So it is interesting to compare the elements. *Orbit 83* is based on only 30 observations spread over 5.9 days, and requires all six  $M$ -coefficients, so that 10 parameters are being determined from 30 observations. This might almost be called a recipe for unreliability. The corresponding one-day orbit, E, with 78 observations and only  $M_0$ ,  $M_1$  and  $M_2$ , should be much more reliable. Comparison shows that the values of  $e$ ,  $\Omega$  and  $M_2$  in orbit 83 are inconsistent with those of orbit E, but the values of  $i$ ,  $\omega$ ,  $M_0$  and  $M_1$  are within the combined s.d. So orbit 83 emerges from the comparison surprisingly well. *Orbit 84* is based on only 16 observations spread over 2.9 days, and requires five  $M$ -coefficients, so that 9 parameters are being determined from 16 observations. This might seem likely to be disastrous, and it is not surprising that the s.d. in inclination is the largest among the 85 orbits. Comparison with the more accurate and more reliable orbit J shows that, although the values of  $i$  and  $M_2$  differ significantly, the values of  $e$ ,  $\Omega$ ,  $(\omega + M_0)$  and  $M_1$  are consistent. So orbit 84, though potentially disastrous, is fairly reliable. *Orbit 85* has 39 observations and covers 2.5 days before decay: six  $M$ -coefficients are needed and  $M_2$  is exceptionally large (8.6 deg/day<sup>2</sup>). All analytical orbit determination programs break down at decay because the perturbations become unlimited, so orbit 85 must inevitably be looked on with suspicion. Comparison with orbit N shows some significant differences, twice the sum of the s.d. on inclination and five times on eccentricity, but good agreement on  $\Omega$  and  $(\omega + M_0)$ . So, although the last three orbits of table 2 were all potentially bad (through lack of observations and proximity to decay), they emerge remarkably well from the test of comparison with the (more accurate) one-day orbits.

On average the standard deviations on orbits 83–85 of table 2 are about three times larger than on the corresponding one-day orbits. The accuracy of the one-day orbits is somewhat better than those of the main orbits without Hewitt camera observations, though not so good as the orbits with Hewitt camera observations.

## 5. ANALYSIS OF VARIATION IN INCLINATION AND ECCENTRICITY AT RESONANCE

If we accept the assumption that the geopotential can be expanded in a double infinite series of tesseral harmonics, ‘lumped’ harmonic coefficients of a particular order (linear functions of individual coefficients) can be determined by analysing the changes that occur in the orbital elements of satellites which experience resonance of that order. The satellite 1971–106A was appreciably perturbed on passing through 14:1, 29:2 and 15:1 resonances, and the effects of these resonances on the orbital inclination and eccentricity have been evaluated.

### 5.1. Theoretical equations for $\beta:\alpha$ resonance

The longitude-dependent geopotential at an exterior point  $(r, \theta, \lambda)$  may be written in normalized form (Kaula 1966) as

$$\frac{\mu_E}{r} \sum_{l=2}^{\infty} \sum_{m=1}^l \left(\frac{R}{r}\right)^l P_l^m(\cos \theta) \{ \bar{C}_{lm} \cos(m\lambda) + \bar{S}_{lm} \sin(m\lambda) \} N_{lm}, \quad (2)$$

where  $r$  is the distance from the Earth’s centre,  $\theta$  is co-latitude,  $\lambda$  is longitude (positive to the east),  $\mu_E$  is the gravitational constant for the Earth (398 601 km<sup>3</sup>/s<sup>2</sup>),  $R$  is the Earth’s equatorial radius

(6378.1 km),  $P_l^m(\cos \theta)$  is the associated Legendre function of order  $m$  and degree  $l$ , and  $\bar{C}_{lm}$  and  $\bar{S}_{lm}$  are the normalized tesseral harmonic coefficients. The normalizing factor  $N_{lm}$  is given by (Kaula 1966)

$$N_{lm}^2 = 2(2l+1)(l-m)!/(l+m)! \quad (3)$$

The rate of change of inclination  $i$  caused by a relevant pair of coefficients,  $\bar{C}_{lm}$  and  $\bar{S}_{lm}$ , near  $\beta:\alpha$  resonance may be written (Allan 1973; Gooding 1979)

$$\frac{di}{dt} = \frac{n(1-e^2)^{-\frac{1}{2}} \left(\frac{R}{a}\right)^l}{\sin i} \bar{F}_{lmp} G_{lpq}(k \cos i - m) \operatorname{Re} [j^{l-m+1} (\bar{C}_{lm} - j\bar{S}_{lm}) \exp \{j(\gamma\Phi - q\omega)\}], \quad (4)$$

where  $\bar{F}_{lmp}$  is Allan's normalized inclination function (Allan 1973),  $G_{lpq}$  is a function of eccentricity  $e$  for which explicit forms have been derived by Gooding (1979),  $\operatorname{Re}$  denotes 'real part of' and  $j = \sqrt{-1}$ . The resonance angle  $\Phi$  is defined by the equation

$$\Phi = \alpha(\omega + M) + \beta(\Omega - \nu), \quad (5)$$

where  $\omega$  is the argument of perigee,  $M$  the mean anomaly,  $\Omega$  the right ascension of the node and  $\nu$  the sidereal angle. The indices  $\gamma$ ,  $q$ ,  $k$  and  $p$  in equation (4) are integers, with  $\gamma$  taking the values 1, 2, 3, ... and  $q$  the values 0,  $\pm 1$ ,  $\pm 2$ , ...; the equations linking  $l$ ,  $m$ ,  $k$  and  $p$  are:  $m = \gamma\beta$ ;  $k = \gamma\alpha - q$ ;  $2p = l - k$ .

At  $\beta:\alpha$  resonance the  $m$ -suffix of a relevant ( $\bar{C}_{lm}$ ,  $\bar{S}_{lm}$ ) pair is given uniquely by the choice of  $\gamma$ . The values of  $l$  to be taken must be such that  $l \geq m$  and  $(l - k)$  is even. The successive coefficients which arise (for given  $\gamma$  and  $q$ ) may usefully be gathered together in a lumped form and written as

$$\bar{C}_m^{q,k} = \sum_l Q_l^{q,k} \bar{C}_{lm}, \quad \bar{S}_m^{q,k} = \sum_l Q_l^{q,k} \bar{S}_{lm}, \quad (6)$$

where  $l$  increases in steps of 2 from its minimum permissible value  $l_0$ , and the  $Q_l^{q,k}$  are functions of inclination that can be taken as constant for a particular satellite, and  $Q_{l_0}^{q,k} = 1$ .

The rate of change of eccentricity  $e$  caused by the  $(l, m)$  harmonic near  $\beta:\alpha$  resonance can be written (Gooding 1979)

$$\frac{de}{dt} = n(1-e^2)^{-\frac{1}{2}} \left(\frac{R}{a}\right)^l \bar{F}_{lmp} G_{lpq} \left\{ \frac{q - \frac{1}{2}(k+q)e^2}{e} \right\} \operatorname{Re} [j^{l-m+1} (\bar{C}_{lm} - j\bar{S}_{lm}) \exp \{j(\gamma\Phi - q\omega)\}], \quad (7)$$

with the same definitions as for equation (4).

As the  $G_{lpq}$  functions (Gooding 1979) are of order  $(\frac{1}{2}le)^{|q|}/(|q|)!$ , it is usually found that for orbits with eccentricity  $< 0.1$  the  $(\gamma, q) = (1, 0)$  terms produce the most important resonance effects on the inclination. For the eccentricity, the relative importance of the terms is largely decided by the value of  $e^{-1}G_{lpq}\{q - \frac{1}{2}(k+q)e^2\}$ , which is of order  $\frac{1}{2}ek$  for  $q = 0$ , of order  $\frac{1}{2}l$  for  $q = \pm 1$  and of order  $\frac{1}{4}l^2e$  for  $q = \pm 2$ . So for the eccentricity the strongest effects are usually caused by the  $(\gamma, q) = (1, 1)$  and  $(1, -1)$  terms, if  $le < 1$ .

However, these rules do not always apply and 1971-106A proves to be somewhat exceptional, because the inclination is quite close to the critical inclination ( $63.4^\circ$ ) and the variation of  $\omega$  is slow, the value of  $\dot{\omega}$  being about 0.5 deg/day. Consequently the  $(\Phi - \omega)$ ,  $\Phi$ , and  $(\Phi + \omega)$  terms in equations (4) and (7) are difficult to separate; when all three are included in the fitting, the correlations between them tend to be high, and there is a danger that the values of the coefficients obtained will have large standard deviations. So, in analysing the three resonances, the possibility arises of dropping one of the three terms to improve the separation of the coefficients. This had to be tested on all three resonances and proved a useful stratagem in two of them. The effects

of including other pairs of  $(\gamma, q)$  values, i.e. higher-order harmonics or subsidiary resonances, are also tested for each of the three resonances analysed.

For each of the three resonances it is necessary to choose the time interval over which the analysis is to be made. If too long a time interval is taken, the orbital parameter ( $i$  or  $e$ ) will not be appreciably affected by the resonance near the ends, and it is better to concentrate the analysis in the region where the variations are strong. The danger of taking too short an interval is that there will not be enough data points. A choice between these extremes must be made. In practice the value of  $\dot{\Phi}$  is used as a guide, and a range of values of  $\dot{\Phi}$  between  $-60$  and  $+60$  deg/day is regarded as the outside limit, but the time interval is reduced if an adequate number of values remain: generally it is advisable to use at least 20 orbits.

## 5.2. Fourteenth-order (14:1) resonance

### 5.2.1 Equations for 14:1 resonance

The most important terms in equation (4) for 14:1 resonance are those with  $\gamma = 1$ , because  $\gamma = 2$  terms are associated with harmonics of order 28 ( $m = \gamma\beta$ ), and should be much smaller than those of order 14. Of the terms with  $\gamma = 1$ , those with  $q = 0, 1$  and  $-1$  are likely to be the most important, since terms with  $q = \pm 2$  have an extra  $e$  factor. With  $\gamma = 1$ ,  $m = \gamma\beta = 14$  and  $k = \gamma\alpha - q = 1 - q$ , and concentrating on terms with  $(\gamma, q) = (1, 0), (1, 1)$  and  $(1, -1)$ , the affixes  $(q, k)$  in equations (6) are  $(0, 1), (1, 0)$  and  $(-1, 2)$ . Writing only the three terms with  $(\gamma, q) = (1, 0), (1, 1)$  and  $(1, -1)$  explicitly and taking  $(1 - e^2)^{-\frac{1}{2}} = 1$ , the theoretical variation of inclination given by equation (4) may be written for 14:1 resonance (Klokočnik 1976; King-Hele *et al.* 1979) as

$$\begin{aligned} \frac{di}{dt} = & \frac{n}{\sin i} \left(\frac{R}{a}\right)^{14} \left[ \frac{R}{a} (14 - \cos i) \bar{F}_{15,14,7} \{ \bar{S}_{14}^{0,1} \sin \Phi + \bar{C}_{14}^{0,1} \cos \Phi \} \right. \\ & + \frac{1}{2} e (14) \bar{F}_{14,14,7} \{ \bar{C}_{14}^{1,0} \sin (\Phi - \omega) - \bar{S}_{14}^{1,0} \cos (\Phi - \omega) \} + \frac{1}{2} e (14 - 2 \cos i) \\ & \left. \times \bar{F}_{14,14,6} \{ \bar{C}_{14}^{-1,2} \sin (\Phi + \omega) - \bar{S}_{14}^{-1,2} \cos (\Phi + \omega) \} + \text{terms in } \left\{ \frac{(\frac{1}{2} l e)^{|q|} \cos (\gamma \Phi - q \omega)}{(|q|)! \sin} \right\} \right]. \quad (8) \end{aligned}$$

The three pairs of lumped coefficients  $\bar{C}_m^{q,k}$  and  $\bar{S}_m^{q,k}$  appearing in equation (8) may be written in terms of the individual geopotential coefficients ( $\bar{C}_{lm}, \bar{S}_{lm}$ ) as indicated in equations (6). Explicitly, with the  $Q_l^{q,k}$  expressed in terms of the  $\bar{F}$  functions, the  $\bar{C}_m^{q,k}$  are (King-Hele *et al.* 1979)

$$\bar{C}_{14}^{0,1} = \bar{C}_{15,14} - \frac{\bar{F}_{17,14,8}}{\bar{F}_{15,14,7}} \left(\frac{R}{a}\right)^2 \bar{C}_{17,14} + \frac{\bar{F}_{19,14,9}}{\bar{F}_{15,14,7}} \left(\frac{R}{a}\right)^4 \bar{C}_{19,14} - \dots, \quad (9)$$

$$\bar{C}_{14}^{1,0} = \bar{C}_{14,14} - \frac{17 \bar{F}_{16,14,8}}{15 \bar{F}_{14,14,7}} \left(\frac{R}{a}\right)^2 \bar{C}_{16,14} + \frac{19 \bar{F}_{18,14,9}}{15 \bar{F}_{14,14,7}} \left(\frac{R}{a}\right)^4 \bar{C}_{18,14} - \dots, \quad (10)$$

$$\bar{C}_{14}^{-1,2} = \bar{C}_{14,14} - \frac{13 \bar{F}_{16,14,7}}{11 \bar{F}_{14,14,6}} \left(\frac{R}{a}\right)^2 \bar{C}_{16,14} + \frac{15 \bar{F}_{18,14,8}}{11 \bar{F}_{14,14,6}} \left(\frac{R}{a}\right)^4 \bar{C}_{18,14} - \dots, \quad (11)$$

and similarly for  $S$ , on replacing  $C$  by  $S$  throughout. The resonance angle  $\Phi$  is given by equation (5) with  $\alpha = 1$  and  $\beta = 14$ .

The most important terms in equation (7), which gives the rate of change of eccentricity, are those with  $(\gamma, q) = (1, 1)$  and  $(1, -1)$ , but for consistency with equation (8) the  $(\gamma, q) = (1, 0)$

terms are also given explicitly. The theoretical equation for eccentricity given by equation (7) may therefore be written for 14 : 1 resonance as (King-Hele *et al.* 1979)

$$\begin{aligned} \frac{de}{dt} = \frac{n}{2} \left(\frac{R}{a}\right)^{14} & \left[ e \left(\frac{R}{a}\right) \bar{F}_{15,14,7} (\bar{S}_{14}^{0,1} \sin \Phi + \bar{C}_{14}^{0,1} \cos \Phi) \right. \\ & - 15 \bar{F}_{14,14,7} \{ \bar{C}_{14}^{1,0} \sin (\Phi - \omega) - \bar{S}_{14}^{1,0} \cos (\Phi - \omega) \} \\ & + 11 \bar{F}_{14,14,6} \{ \bar{C}_{14}^{-1,2} \sin (\Phi + \omega) - \bar{S}_{14}^{-1,2} \cos (\Phi + \omega) \} \\ & \left. + \text{terms in } \left[ \frac{(\frac{1}{2}l)^{|q|} e^{|q|-1}}{(|q|)!} \left\{ q - \frac{1}{2}(k+q) e^2 \right\} \frac{\cos (\gamma\Phi - q\omega)}{\sin (\gamma\Phi - q\omega)} \right] \right], \end{aligned} \quad (12)$$

where the  $\bar{C}_{14}^{q,k}$  and  $\bar{S}_{14}^{q,k}$  are given by equations (9) to (11).

### 5.2.2. Analysis of inclination, $i$

Cosmos 462 passed through exact 14th-order resonance at MJD 41 659 (1972 December 8). The effect of this resonance on the inclination has been analysed over a period of about 2 months either side of exact resonance by using the THROE computer program developed by Gooding (1971), which fits the values of  $i$  with equation (4) in integrated form by the least-squares method. During this time there were 27 values of inclination available for analysis, 10 values from the PROP orbits in table 2 and 17 values from orbits supplied by the U.S. Navy. All values of inclination were cleared of lunisolar and zonal harmonic perturbations by using the computer program PROD (Cook 1973) with one-day integration steps; for the orbits of table 2, the  $J_{2,2}$  perturbations were also removed. The U.S. Navy values were initially given standard deviations of  $0.003^\circ$  and the PROP values were given their quoted standard deviations from table 2. Four of the PROP values had their standard deviations increased to  $0.0005^\circ$  to allow for the neglected effect of Earth tides; one of the U.S. Navy values was discarded because it was inaccurate and another, that at MJD 41 612, had its s.d. increased by a factor of two.

The remaining 26 values of inclination were fitted with equation (8) by using THROE, i.e. with  $(\gamma, q) = (1, 0)$ ,  $(1, 1)$  and  $(1, -1)$ . The coefficients  $(\bar{C}, \bar{S})_{14}^{q,k}$  in equation (8) were undetermined in this fitting, i.e. the standard deviations are of the same order as the values of the coefficients. This was to be expected because of the correlations mentioned earlier (§5.1) and because there were only 26 values being fitted, scarcely enough to allow a good determination of the seven coefficients (the six harmonic coefficients and the initial value of inclination).

So the values were then fitted with  $(\gamma, q) = (1, 0)$  only. The values of lumped harmonics obtained were

$$10^9 \bar{C}_{14}^{0,1} = 62 \pm 9, \quad 10^9 \bar{S}_{14}^{0,1} = 1 \pm 19, \quad (13)$$

with  $\epsilon = 1.66$  ( $\epsilon$  is as defined in §3). A further run, with  $(\gamma, q) = (1, 0)$  and  $(2, 0)$ , offered no advantage: the  $(2, 0)$  coefficients were undetermined and  $\epsilon$  increased slightly. The values of the coefficients in equation (13) are satisfactory in that they provide an acceptable fitting, but they include the effects of the neglected  $(1, 1)$  and  $(1, -1)$  terms. Values of individual 14th-order coefficients (King-Hele *et al.* 1979) indicated that the values of  $\bar{C}_{14}^{0,1}$  and  $\bar{S}_{14}^{0,1}$  for 1971–106A should be approximately  $9 \times 10^9$  and  $-25 \times 10^{-9}$ . These values are of the same order as those in equation (13) but differ sufficiently to suggest that the absorption of the  $(1, 1)$  and  $(1, -1)$  terms does affect the values obtained.

Next the variation of inclination given by using the values  $10^9 \bar{C}_{14}^{0,1} = 9$  and  $10^9 \bar{S}_{14}^{0,1} = -25$  was calculated with the aid of THROE. It was found that the variation in inclination was extremely

small, never more than  $\pm 0.0008^\circ$ . The  $(1, 0)$  terms were therefore discarded and the values of inclination fitted with  $(\gamma, q) = (1, 1)$  and  $(1, -1)$ . The results were fairly satisfactory, with  $\epsilon = 1.5$  and standard deviations about  $\frac{1}{3}$  of the values of the coefficients.

The next point to be considered was the possibility that  $(\gamma, q) = (1, 2)$  and  $(1, -2)$  terms might have an appreciable effect. Values of  $(\bar{C}, \bar{S})_{14}^{2,-1}$  and  $(\bar{C}, \bar{S})_{14}^{-2,3}$  were calculated from the values of individual 14th-order coefficients from King-Hele *et al.* (1979), and the variation of inclination due to the  $(\gamma, q) = (1, 2)$  and  $(1, -2)$  terms was calculated by using THROE. These terms produced an appreciable change in inclination at resonance, about  $0.0015^\circ$ . The raw values of inclination were therefore modified by subtracting the effect of the  $(1, 2)$  and  $(1, -2)$  terms as given by this calculation and a new fitting of  $(\gamma, q) = (1, 1)$  and  $(1, -1)$  terms was made.

The values obtained were

$$\left. \begin{aligned} 10^9 \bar{C}_{14}^{1,0} &= -399 \pm 218, & 10^9 \bar{S}_{14}^{1,0} &= 394 \pm 158, \\ 10^9 \bar{C}_{14}^{-1,2} &= 101 \pm 97, & 10^9 \bar{S}_{14}^{-1,2} &= 412 \pm 152, \end{aligned} \right\} \quad (14)$$

with  $\epsilon = 1.48$ . The fitting is quite good, the curve being shown as a full line in figure 5.

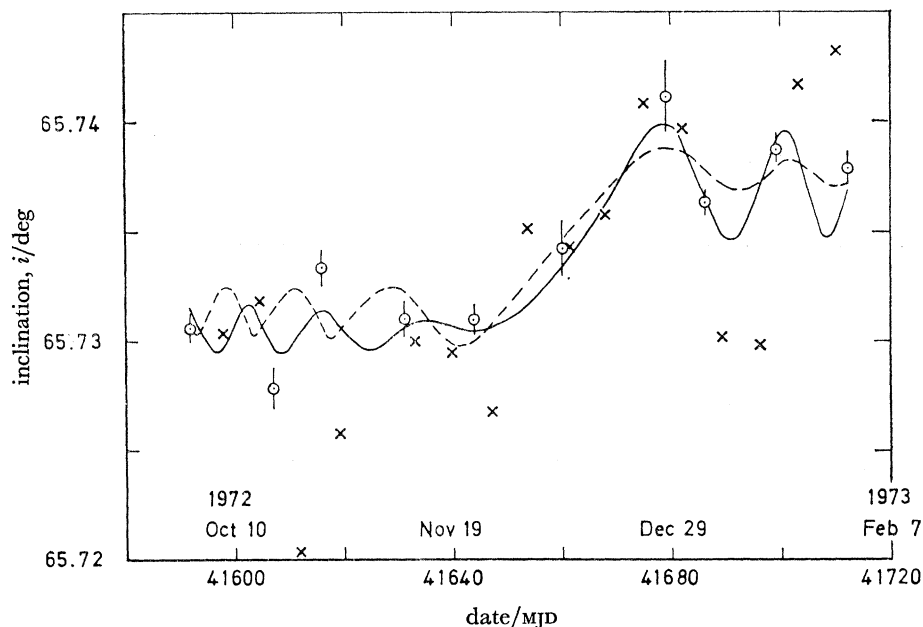


FIGURE 5. Variation of inclination at 14th-order resonance.  $\odot$ , from R.A.E. orbits;  $\times$ , from U.S. Navy orbits. —, THROE fitting of  $i$  alone; ----, SIMRES fitting of  $i$  and  $e$  together.

The values (14) are not entirely satisfactory because of their large standard deviations, which stem from the strong correlations between coefficients – for example the correlation between  $\bar{C}_{14}^{1,0}$  and  $\bar{S}_{14}^{-1,2}$  is  $-0.953$ . So a better solution is likely to be possible from the simultaneous fit of inclination and eccentricity by using the SIMRES computer program (Gooding 1979). This will be discussed after the analysis of the values of eccentricity.

### 5.2.3. Analysis of eccentricity, $e$

The effect of the 14:1 resonance on the eccentricity of the orbit of 1971-106A has been analysed over the same period as the inclination, i.e. about 2 months either side of exact resonance, from the

same 27 orbits. The U.S. Navy values were given standard deviations of 0.00008 and the PROP values were given the standard deviations quoted in table 2. Three of the PROP values of eccentricity had their standard deviations increased to 0.000008 to allow for the neglected effect of Earth tides, and the U.S. Navy value dropped from the inclination analysis because of inaccuracy was also omitted here, for the same reason. All values of eccentricity were cleared of lunisolar and zonal harmonic perturbations by using the PROD computer program as with the inclination values.

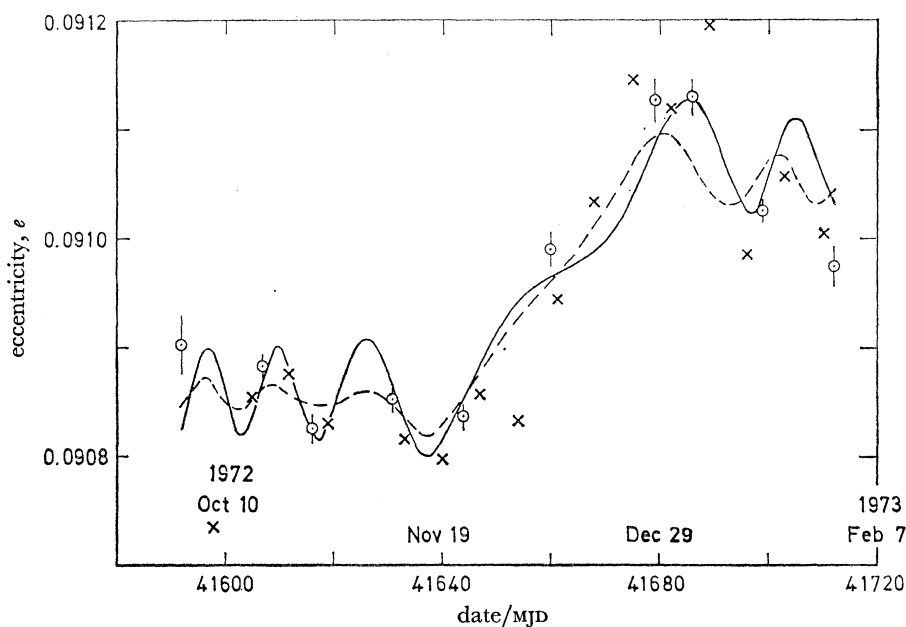


FIGURE 6. Variation of eccentricity at 14th-order resonance.  $\odot$ , from R.A.E. orbits;  $\times$ , from U.S. Navy orbits. —, THROE fitting of  $e$  alone; ---, SIMRES fitting of  $i$  and  $e$  together.

After the first THROE fitting, with equations (12) but omitting  $(\gamma, q) = (1, 0)$  terms, it was apparent that the U.S. Navy values of eccentricity suffered a bias relative to the PROP values. This mismatch between U.S. Navy and PROP values of  $e$  has arisen previously (Walker 1975), and was attributed to an inconsistency in restoring the odd-zonal harmonic perturbation to the U.S. Navy values. Since the perturbation to  $e$  is of the form  $K \sin \omega$ , where  $K$  is a constant, the simplest procedure for correcting the bias is to subtract an expression of this form from the values of  $e$ , the value of  $K$  being chosen empirically to minimize the bias. Here the quantity  $0.00015 \sin \omega$  was subtracted from each of the U.S. Navy values of  $e$ .

The first THROE run after making this modification showed that the first PROP value of  $e$ , at MJD 41 592, fitted badly and its s.d. was increased by a factor of  $\sqrt{10}$ . The resulting THROE run for  $(\gamma, q) = (1, 1), (1, -1)$  gave  $\epsilon = 1.5$  and values of the coefficients with standard deviations not much smaller than the values. Next the effects of the terms  $(\gamma, q) = (1, 2), (1, -2)$  were calculated by using values of the individual coefficients from King-Hele *et al.* (1979). The variation in  $e$  due to these terms was appreciable, about 0.00003, so the values of  $e$  were cleared of this perturbation, and refitted with THROE. The resulting values of the coefficients were

$$\left. \begin{aligned} 10^9 \bar{C}_{14}^{1,0} &= -139 \pm 247, & 10^9 \bar{S}_{14}^{1,0} &= 678 \pm 226, \\ 10^9 \bar{C}_{14}^{-1,2} &= -733 \pm 154, & 10^9 \bar{S}_{14}^{-1,2} &= -271 \pm 165, \end{aligned} \right\} \quad (15)$$

with  $\epsilon = 1.50$ . In this fitting the density scale height  $H$  was taken as 42 km, the value appropriate for a height  $\frac{3}{2}H$  above perigee. (Values of 44 and 46 km were also tried, but were less satisfactory.) The fitting is quite good, the curve being shown as a full line in figure 6, but the standard deviations of the values are too large to be regarded as satisfactory, again because of the high correlation between coefficients: for example the correlation between  $\bar{S}_{14}^{1,0}$  and  $\bar{C}_{14}^{-1,2}$  is 0.955. Therefore a simultaneous fitting with  $i$  is required and is discussed in the following section.

#### 5.2.4. Inclination and eccentricity fitted simultaneously

The values of inclination and eccentricity fitted separately by THROE were next fitted simultaneously by least squares with the aid of the computer program SIMRES. This program combines the results from a number of THROE runs and produces a single set of coefficients to fit the data. The program allows a choice of weighting, so that the contributing THROE runs can be given more or less weight according to their accuracy of fit, indicated by the value of  $\epsilon$ .

Here the final THROE runs for  $i$  and  $e$  were combined and no weighting factor was applied because  $\epsilon$  was 1.5 in both contributing THROE runs. The SIMRES fittings are shown in figures 5 and 6 by broken lines and the values of the coefficients given by SIMRES are

$$\left. \begin{aligned} 10^9 \bar{C}_{14}^{1,0} &= 17 \pm 59, & 10^9 \bar{S}_{14}^{1,0} &= -137 \pm 35, \\ 10^9 \bar{C}_{14}^{-1,2} &= -186 \pm 16, & 10^9 \bar{S}_{14}^{-1,2} &= 66 \pm 42. \end{aligned} \right\} \quad (16)$$

The standard deviations of the values in (16) are considerably smaller than in (14) or (15), and the values should also be more reliable because the number of values being fitted is doubled. This conclusion is confirmed by figures 5 and 6, which show that for both  $i$  and  $e$  the SIMRES fitting looks just as good as – or perhaps better than – the individual fittings. The values (16) differ from the corresponding values in (14) and (15) by between 0.5 and 3.2 times the sum of the standard deviations. The individual differences for each coefficient, expressed as multiples of the sum of the standard deviations, are as follows:

	$\bar{C}_{14}^{1,0}$	$\bar{S}_{14}^{1,0}$	$\bar{C}_{14}^{-1,2}$	$\bar{S}_{14}^{-1,2}$
$i$	1.5	2.8	2.5	1.8
$e$	0.5	3.1	3.2	1.6

From this table it might be expected that the values of  $\bar{C}_{14}^{1,0}$  and  $\bar{S}_{14}^{-1,2}$  would be more reliable than the other two.

In the recent evaluation of individual 14th-order harmonics in the geopotential (King-Hele *et al.* 1979), the lumped harmonic values in equation (16) were used in the solutions for harmonics of order 14 and even degree. It was found that the  $\bar{C}_{14}^{1,0}$  and  $\bar{S}_{14}^{-1,2}$  values in equation (16) made a useful contribution to the solution, yielding weighted residuals of 0.04 and 0.71 respectively in the five-coefficient solution quoted in table 7 of King-Hele *et al.* (1979). The  $\bar{S}_{14}^{1,0}$  and  $\bar{C}_{14}^{-1,2}$  values in equation (16), however, did not fit so well and their standard deviations were increased by factors of 5 and 10 respectively: even then, the weighted residuals for these two coefficients in the five-coefficient solution quoted in table 7 of King-Hele *et al.* (1979) are  $-1.17$  and  $-1.14$  respectively. This confirms the indication that the values of  $\bar{C}_{14}^{1,0}$  and  $\bar{S}_{14}^{-1,2}$  in equation (16) are more reliable than the other two.

#### 5.3. 29:2 resonance

The changes in inclination and eccentricity at 29:2 resonance are expected to be only  $\frac{1}{3}$  as large as at 14:1 resonance, because the values of the  $\bar{C}_{im}$  are likely to be only  $\frac{1}{4}$  as large, and the



resonance is faster because  $\ddot{\Phi} \approx \alpha \dot{M}$  is twice as large. So the chances of successful analysis are poorer. However, the analysis needs to be made to assess the overall change in  $i$  at resonance.

### 5.3.1. Equations for 29:2 resonance

The most important terms in equation (4) for 29:2 resonance are those with  $\gamma = 1$  and  $q = 0, 1$  and  $-1$ . The  $\gamma = 2$  terms are associated with harmonics of order 58 ( $m = \gamma\beta$ ), which should be much smaller than those of order 29; and terms with  $q = \pm 2$  have an extra  $e$  factor.

For the 29:2 resonance with  $\gamma = 1$ ,  $m = \gamma\beta = 29$  and  $k = \gamma\alpha - q = 2 - q$ , so that the affixes  $(q, k)$  in equation (6) are  $(0, 2)$ ,  $(1, 1)$  and  $(-1, 3)$  when  $q = 0, 1$  and  $-1$  respectively. Writing only the three terms with  $(\gamma, q) = (1, 0)$ ,  $(1, 1)$  and  $(1, -1)$  explicitly, the theoretical variation of inclination given by equation (4) may be written for 29:2 resonance (Klokočník 1976; Walker 1977) as

$$\begin{aligned} \frac{di}{dt} = & \frac{n}{\sin i} \left(\frac{R}{a}\right)^{29} \left[ \frac{R}{a} (29 - 2 \cos i) \bar{F}_{30, 29, 14} \{ \bar{S}_{29}^{0, 2} \sin \Phi + \bar{C}_{29}^{0, 2} \cos \Phi \} \right. \\ & + 16e(29 - \cos i) \bar{F}_{29, 29, 14} \{ \bar{C}_{29}^{1, 1} \sin(\Phi - \omega) - \bar{S}_{29}^{1, 1} \cos(\Phi - \omega) \} \\ & + 12e(29 - 3 \cos i) \bar{F}_{29, 29, 13} \{ \bar{C}_{29}^{-1, 3} \sin(\Phi + \omega) - \bar{S}_{29}^{-1, 3} \cos(\Phi + \omega) \} \\ & \left. + \text{terms in } \left[ \frac{(\frac{1}{2}le)^{|q|} \cos(\gamma\Phi - q\omega)}{(|q|)! \sin} \right] \right]. \end{aligned} \quad (17)$$

The three pairs of lumped coefficients  $\bar{C}_m^{q, k}$  and  $\bar{S}_m^{q, k}$  appearing in equation (17) may be written in terms of the individual geopotential coefficients  $(\bar{C}_{lm}, \bar{S}_{lm})$  as indicated in equations (6). Explicitly, with the  $Q_m^{q, k}$  expressed in terms of the  $\bar{F}$  functions, the  $\bar{C}_m^{q, k}$  are (Walker 1977)

$$\bar{C}_{29}^{0, 2} = \bar{C}_{30, 29} - \frac{\bar{F}_{32, 29, 15}}{\bar{F}_{30, 29, 14}} \left(\frac{R}{a}\right)^2 \bar{C}_{32, 29} + \frac{\bar{F}_{34, 29, 16}}{\bar{F}_{30, 29, 14}} \left(\frac{R}{a}\right)^4 \bar{C}_{34, 29} - \dots, \quad (18)$$

$$\bar{C}_{29}^{1, 1} = \bar{C}_{29, 29} - \frac{17\bar{F}_{31, 29, 15}}{16\bar{F}_{29, 29, 14}} \left(\frac{R}{a}\right)^2 \bar{C}_{31, 29} + \frac{18\bar{F}_{33, 29, 16}}{16\bar{F}_{29, 29, 14}} \left(\frac{R}{a}\right)^4 \bar{C}_{33, 29} - \dots, \quad (19)$$

$$\bar{C}_{29}^{-1, 3} = \bar{C}_{29, 29} - \frac{13\bar{F}_{31, 29, 14}}{12\bar{F}_{29, 29, 13}} \left(\frac{R}{a}\right)^2 \bar{C}_{31, 29} + \frac{14\bar{F}_{33, 29, 15}}{12\bar{F}_{29, 29, 13}} \left(\frac{R}{a}\right)^4 \bar{C}_{33, 29} - \dots, \quad (20)$$

and similarly for  $S$ , on replacing  $C$  by  $S$  throughout. The resonance angle  $\Phi$  is given by equation (5) with  $\alpha = 2$  and  $\beta = 29$ .

For the 29:2 resonance, the theoretical variation of eccentricity given by equation (7) may be written in terms of the same  $(\bar{C}_m^{q, k}, \bar{S}_m^{q, k})$  as (Walker 1977)

$$\begin{aligned} \frac{de}{dt} = & n \left(\frac{R}{a}\right)^{29} \left[ -e \left(\frac{R}{a}\right) \bar{F}_{30, 29, 14} (\bar{S}_{29}^{0, 2} \sin \Phi + \bar{C}_{29}^{0, 2} \cos \Phi) \right. \\ & - 16\bar{F}_{29, 29, 14} \{ \bar{C}_{29}^{1, 1} \sin(\Phi - \omega) - \bar{S}_{29}^{1, 1} \cos(\Phi - \omega) \} \\ & + 12\bar{F}_{29, 29, 13} \{ \bar{C}_{29}^{-1, 3} \sin(\Phi + \omega) - \bar{S}_{29}^{-1, 3} \cos(\Phi + \omega) \} \\ & \left. + \text{terms in } \left[ \frac{(\frac{1}{2}l)^{|q||q|-1}}{(|q|)!} \{ q - \frac{1}{2}(k+q) e^2 \} \frac{\cos}{\sin}(\gamma\Phi - q\omega) \right] \right]. \end{aligned} \quad (21)$$

Three terms are given explicitly in equation (21), those with  $(\gamma, q) = (1, 0)$ ,  $(1, 1)$  and  $(1, -1)$ . The main terms are expected to be those with  $(\gamma, q) = (1, 1)$  and  $(1, -1)$  but the  $(\gamma, q) = (1, 0)$  term is also given explicitly for consistency with equation (17).

5.3.2. *Analysis of inclination,  $i$* 

The inclination of Cosmos 462 was analysed at the time of 29:2 resonance by using 21 values of inclination, seven values being from the PROP orbits in table 2 and 14 values from orbits supplied by the U.S. Navy. The analysis extended to nearly 2 months either side of exact 29:2 resonance, which occurred at MJD 42012 (1973 November 26). All values of inclination were cleared of lunisolar and zonal harmonic perturbations by using the PROD program (Cook 1973) with one-day integration steps and, for the seven values from table 2, the  $J_{2,2}$  perturbation. The U.S. Navy values were given standard deviations of  $0.003^\circ$  and the PROP values were given their quoted standard deviations in table 2.

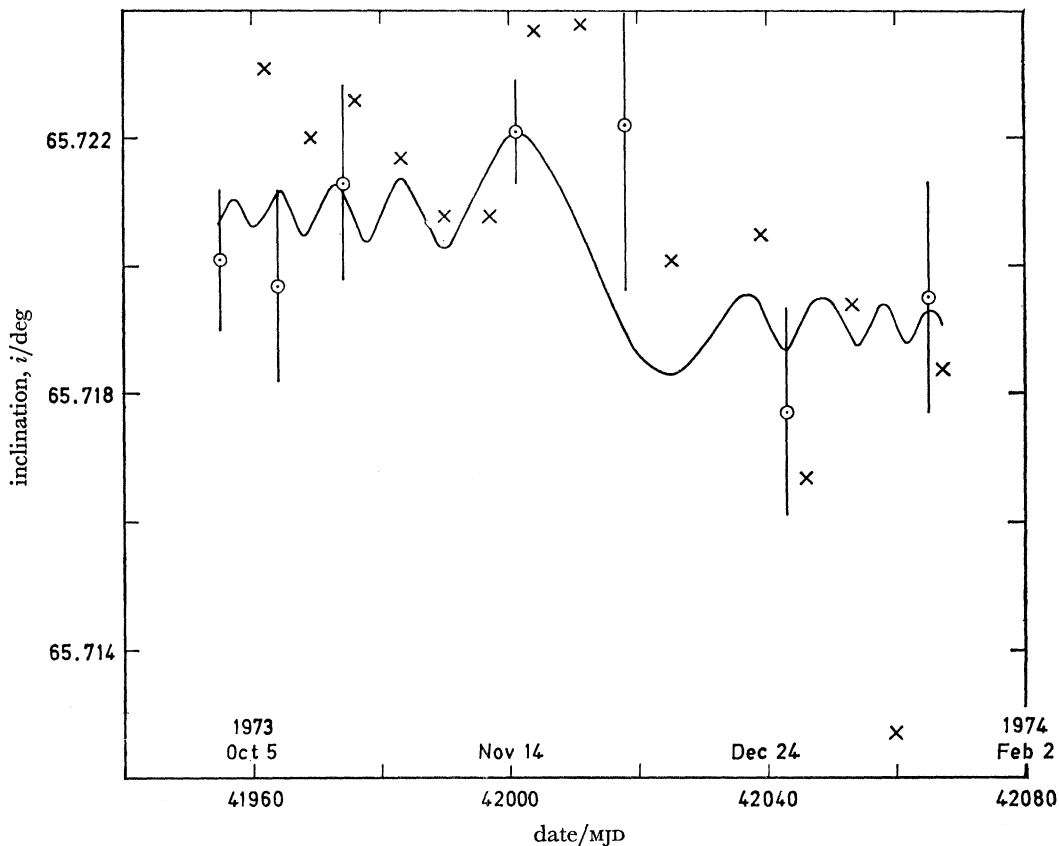


FIGURE 7. Variation of inclination at 29:2 resonance.  $\circ$ , from R.A.E. orbits;  $\times$ , from U.S. Navy orbits. —, THROE fitting of  $i$ .

The 21 values of inclination were then fitted with equation (17) with the aid of THROE, i.e. with  $(\gamma, q) = (1, 0)$ ,  $(1, 1)$  and  $(1, -1)$ . All the  $(\bar{C}, \bar{S})_{29}^{0,k}$  coefficients in equation (17) were undetermined in this fitting, but the fit did reveal that the U.S. Navy values were all too large: discrepancies of this kind have been found previously (Hiller 1972; King-Hele 1974; Walker 1975) and are due to differences in definition in the U.S. Navy orbits. The difficulty is avoided by making a (constant) empirical change in the U.S. Navy values and here they were all reduced by  $0.004^\circ$ . The standard deviations on one PROP value of inclination, at MJD 42018, and one U.S. Navy, at MJD 42060, were increased by a factor of two. The program was then re-run, but with similar

results: all seven coefficients were undetermined, as was expected because of the correlations mentioned earlier (see §5.1) and also because there were only 21 values being fitted.

The values were then fitted with  $(\gamma, q) = (1, 0)$  only, because at this resonance  $\epsilon = 0.065$  and therefore the  $(1, 1)$  and  $(1, -1)$  terms should not have so much effect. The values obtained were

$$10^9 \bar{C}_{29}^{0,2} = -90 \pm 74, \quad 10^9 \bar{S}_{29}^{0,2} = -127 \pm 39, \quad (22)$$

with  $\epsilon = 0.689$ . These values were obtained after the  $M_2$  values on the orbits had been changed (see §5.3.3). The fitted curve is shown as a full line in figure 7. The values in equation (22) should be useful in the future in determining the individual coefficients of 29th order and even degree.

Even though the numerical values of the lumped harmonics were not particularly accurate, the fitting is useful in showing that there was an overall decrease of  $0.002^\circ$  in passing through 29:2 resonance and in providing end points for the analysis of atmospheric rotation (see §6).

### 5.3.3. Analysis of eccentricity, $e$

The effect of the 29:2 resonance on the eccentricity was analysed using values of  $e$  from the same 21 orbits. All values of  $e$  were cleared of lunisolar and zonal harmonic perturbations with the aid of PROD. The PROD values were given the standard deviations quoted in table 2 and the U.S. Navy values were given standard deviations of 0.00008. The density scale height was taken as 42 km.

After the first THROE fitting with equation (21), i.e. with  $(\gamma, q) = (1, 0)$ ,  $(1, 1)$  and  $(1, -1)$ , it was again apparent that the U.S. Navy values of  $e$  suffered a bias relative to the PROD values. This bias was corrected as previously (see §5.2.3) by subtracting an expression of the form  $K \sin \omega$ , where  $K$  is a constant chosen empirically to minimize the bias and taken here as 0.00045. The subsequent THROE fitting with  $(\gamma, q) = (1, 0)$ ,  $(1, 1)$  and  $(1, -1)$  yielded undetermined values of the coefficients and they also had high correlations: it was obviously not possible to determine seven coefficients from 21 values.

In the course of the fitting of  $e$ , a source of error in the technique for using the THROE program became apparent. The correction of eccentricity to allow for the effects of atmospheric drag between one orbit and the next is calculated in THROE by using the value of  $M_2$  for the first of the two orbits, which is assumed to apply over the time interval between them. However, it is not correct to assume that the value of  $M_2$  for the first orbit remains valid over the time interval between the two orbits, often 7 days: for the PROD orbits the value of  $M_2$  usually applies over about 3 days either side of epoch, and for the U.S. Navy orbits for approximately 5 days before epoch. So the technique hitherto used was modified, and the value of  $M_2$  at the  $n$ th epoch was taken as  $\frac{1}{2}\{(M_2)_{n+1} - (M_2)_n\}/(t_{n+1} - t_n)$ . This ensures that the integrated effect of air drag between epoch  $t_n$  and epoch  $t_{n+1}$  is correctly represented. This correction had an important effect in the eccentricity runs, but no significant effect for inclination, where the atmospheric corrections are very small; however, the values of  $M_2$  were changed for  $i$ , for consistency between the fittings.

After changing the values of  $M_2$ , the values of  $e$  to be fitted, when adjusted for the effects of atmospheric drag by THROE, showed very little variation, all the values being within 0.00015 of the value 0.06900. So the chances of obtaining good lumped values of 29th-order harmonics were unpromising. Fitting with  $(\gamma, q) = (1, 1)$  and  $(1, -1)$  gave quite undetermined values, so it was necessary to fit with  $(\gamma, q) = (1, 1)$  only, or  $(\gamma, q) = (1, -1)$  only. These alternative fittings were very similar with  $\epsilon = 1.33$  and 1.30 respectively, but the latter seems marginally preferable because it fits the PROD values of eccentricity better. The  $(\gamma, q) = (1, -1)$  fitting is shown in figure 8.

The values obtained for the coefficients in this  $(1, -1)$  fitting are  $(907 \pm 325) \times 10^{-9}$  and  $(-463 \pm 163) \times 10^{-9}$ : these are nominally values of  $\bar{C}_{29}^{-1,3}$  and  $\bar{S}_{29}^{-1,3}$  respectively, but they include the effects of  $\bar{C}_{29}^{1,1}$  and  $\bar{S}_{29}^{1,1}$ . However the results, even if the interference from  $\bar{C}_{29}^{1,1}$  and  $\bar{S}_{29}^{1,1}$  is slight, are not accurate enough to give numerical values useful in determining individual 29th-order coefficients. In other words, the variation in eccentricity over the region of 29:2 resonance is too small to yield good values of lumped coefficients because the orbit of 1971-106A is strongly affected by drag and the effect of resonance does not last long enough for an appreciable change in  $e$  to build up.

Since the change in  $e$  is not large enough to give values of lumped coefficients, there was no purpose in making a SIMRES fitting of  $i$  and  $e$  together.

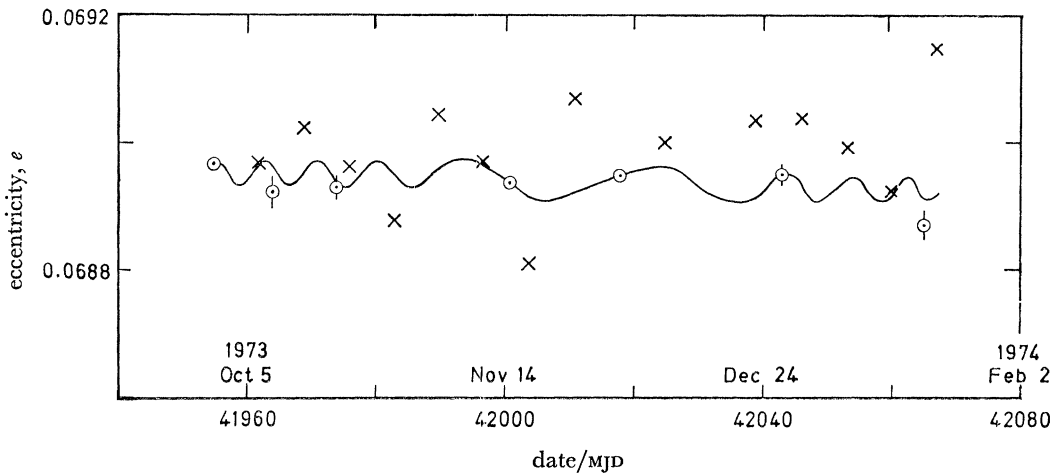


FIGURE 8. Variation of eccentricity at 29:2 resonance.  $\odot$ , from R.A.E. orbits;  $\times$ , from U.S. Navy orbits. —, THROE fitting of  $e$ .

#### 5.4. Fifteenth-order (15:1) resonance

##### 5.4.1. Equations for 15:1 resonance

As for the two preceding resonances, the most important terms in equation (4) for 15:1 resonance are likely to be those with  $\gamma = 1$ , because  $\gamma = 2$  terms are associated with harmonics of order 30 ( $m = \gamma\beta$ ), and should be considerably smaller than those of order 15. Again the most important terms with  $\gamma = 1$  are those with  $q = 0, 1$  and  $-1$ , since  $q = 2$  terms have an extra  $e$  factor. Therefore, with  $\gamma = 1$ ,  $m = 15$  and  $k = \gamma\alpha - q = 1 - q$ , and concentrating on terms with  $(\gamma, q) = (1, 0), (1, 1)$  and  $(1, -1)$ , the affixes  $(q, k)$  in equations (6) are  $(0, 1), (1, 0)$  and  $(-1, 2)$ . So, writing only the three terms with  $(\gamma, q) = (1, 0), (1, 1)$  and  $(1, -1)$  explicitly, equation (4) giving the theoretical variation of inclination may be written for 15:1 resonance as

$$\begin{aligned} \frac{di}{dt} = & \frac{n}{\sin i} \left(\frac{R}{a}\right)^{15} \left[ (15 - \cos i) \bar{F}_{15,15,7} \{ \bar{C}_{15}^{0,1} \sin \Phi - \bar{S}_{15}^{0,1} \cos \Phi \} \right. \\ & + \frac{1}{2} e (15) \left(\frac{R}{a}\right) \bar{F}_{16,15,8} \{ \bar{S}_{15}^{1,0} \sin (\Phi - \omega) + \bar{C}_{15}^{1,0} \cos (\Phi - \omega) \} \\ & + \frac{1}{2} e (15 - 2 \cos i) \left(\frac{R}{a}\right) \bar{F}_{16,15,7} \{ \bar{S}_{15}^{-1,2} \sin (\Phi + \omega) + \bar{C}_{15}^{-1,2} \cos (\Phi + \omega) \} \\ & \left. + \text{terms in } \left\{ \frac{(\frac{1}{2}e)^{|q|}}{(|q|)!} \cos (\gamma\Phi - q\omega) \right\} \right]. \end{aligned} \quad (23)$$

The three pairs of lumped coefficients  $\bar{C}_m^{q,k}$  and  $\bar{S}_m^{q,k}$  appearing in equation (23) may be written in terms of the individual geopotential coefficients ( $\bar{C}_{lm}$ ,  $\bar{S}_{lm}$ ) as indicated in equation (6). Explicitly, with the  $Q_l^{q,k}$  expressed in terms of the  $\bar{F}$  functions, the  $\bar{C}_m^{q,k}$  are

$$\bar{C}_{15}^{0,1} = \bar{C}_{15,15} - \frac{\bar{F}_{17,15,8}}{\bar{F}_{15,15,7}} \left(\frac{R}{a}\right)^2 \bar{C}_{17,15} + \frac{\bar{F}_{19,15,9}}{\bar{F}_{15,15,7}} \left(\frac{R}{a}\right)^4 \bar{C}_{19,15} - \dots, \quad (24)$$

$$\bar{C}_{15}^{1,0} = \bar{C}_{16,15} - \frac{19\bar{F}_{18,15,9}}{17\bar{F}_{16,15,8}} \left(\frac{R}{a}\right)^2 \bar{C}_{18,15} + \frac{21\bar{F}_{20,15,10}}{17\bar{F}_{16,15,8}} \left(\frac{R}{a}\right)^4 \bar{C}_{20,15} - \dots, \quad (25)$$

$$\bar{C}_{15}^{-1,2} = \bar{C}_{16,15} - \frac{15\bar{F}_{18,15,8}}{13\bar{F}_{16,15,7}} \left(\frac{R}{a}\right)^2 \bar{C}_{18,15} + \frac{17\bar{F}_{20,15,9}}{13\bar{F}_{16,15,7}} \left(\frac{R}{a}\right)^4 \bar{C}_{20,15} - \dots, \quad (26)$$

and similarly for  $S$ , on replacing  $C$  by  $S$  throughout. The resonance angle  $\Phi$  is given by equation (5) with  $\alpha = 1$  and  $\beta = 15$ .

For the 15:1 resonance, the theoretical variation of eccentricity given by equation (7) may be written in terms of the same ( $\bar{C}_m^{q,k}$ ,  $\bar{S}_m^{q,k}$ ) as

$$\begin{aligned} \frac{de}{dt} = & \frac{n}{2} \left(\frac{R}{a}\right)^{15} \left[ e\bar{F}_{15,15,7} (\bar{C}_{15}^{0,1} \sin \Phi - \bar{S}_{15}^{0,1} \cos \Phi) \right. \\ & - 17 \left(\frac{R}{a}\right) \bar{F}_{16,15,8} \{ \bar{S}_{15}^{1,0} \sin(\Phi - \omega) + \bar{C}_{15}^{1,0} \cos(\Phi - \omega) \} \\ & + 13 \left(\frac{R}{a}\right) \bar{F}_{16,15,7} \{ \bar{S}_{15}^{-1,2} \sin(\Phi + \omega) + \bar{C}_{15}^{-1,2} \cos(\Phi + \omega) \} \\ & \left. + \text{terms in } \left[ \frac{(\frac{1}{2}l)^{|q|} e^{|q|-1}}{(|q|)!} \{ q - \frac{1}{2}(k+q) e^{2i} \}_{\cos}^{\gamma} \sin(\gamma\Phi - q\omega) \right] \right]. \quad (27) \end{aligned}$$

Three terms are given explicitly in equation (27), those with  $(\gamma, q) = (1, 0)$ ,  $(1, 1)$  and  $(1, -1)$ . The main terms, as with the previous two resonances, are expected to be those with  $(\gamma, q) = (1, 1)$  and  $(1, -1)$ , but the  $(\gamma, q) = (1, 0)$  term is given for consistency with equation (23).

#### 5.4.2. Analysis of inclination, $i$

At the time of 15th-order resonance, nine PROP orbits from table 2 and 13 U.S. Navy orbits were available for analysis. The analysis covers a period of approximately 2 months before and 1 month after the date of exact 15:1 resonance, MJD 42 302 (1974 September 12). All values of inclination were cleared of lunisolar and zonal harmonic perturbations by using the PROP program (Cook 1973) with one-day integration steps; and the nine values from table 2 were cleared of the  $J_{2,2}$  perturbation. The U.S. Navy values were given standard deviations of 0.003° and the PROP values were given their quoted standard deviations in table 2.

The 22 values of inclination were fitted with equation (23) by using THROE, i.e. with  $(\gamma, q) = (1, 0)$ ,  $(1, 1)$  and  $(1, -1)$ . The coefficients ( $\bar{C}$ ,  $\bar{S}$ ) $_{15}^{q,k}$  in equation (23) were undetermined in this fitting, so the values were then fitted with just  $(\gamma, q) = (1, 0)$ . For this fitting the U.S. Navy value at MJD 42 333 was dropped because it was inaccurate and the  $M_2$  values on the orbits were changed as for the 29:2 resonance (see §5.3.3). The values obtained were

$$10^9 \bar{C}_{15}^{0,1} = -36 \pm 21, \quad 10^9 \bar{S}_{15}^{0,1} = 9 \pm 17, \quad (28)$$

with  $\epsilon = 1.102$ . The fitted curve is shown as a full line in figure 9. These values of ( $\bar{C}$ ,  $\bar{S}$ ) $_{15}^{0,1}$  are quite small and consequently not well determined. Previous evaluations of 15th-order coefficients (King-Hele, Walker & Gooding 1975*b*) indicate that at inclinations near 65° the

values of both  $\bar{C}_{15}^{0,1}$  and  $\bar{S}_{15}^{0,1}$  are near zero, and of order  $(0 \pm 20) \times 10^{-9}$ ; the variation of  $\bar{C}_{15}^{0,1}$  and  $\bar{S}_{15}^{0,1}$  near  $65^\circ$  is not very well defined in King-Hele *et al.* (1975*b*) because the only value available near  $65^\circ$  – Cosmos 387 at  $62.9^\circ$  – may not be entirely reliable, as the data on which it is based are very limited.

As the  $(\bar{C}, \bar{S})_{15}^{0,1}$  coefficients are small for 1971–106A, it was worth fitting the inclination values with  $(\gamma, q) = (1, 1)$  and  $(1, -1)$ . The values obtained were

$$\left. \begin{aligned} 10^9 \bar{C}_{15}^{1,0} &= 29 \pm 83, & 10^9 \bar{S}_{15}^{1,0} &= 196 \pm 142, \\ 10^9 \bar{C}_{15}^{-1,2} &= 116 \pm 124, & 10^9 \bar{S}_{15}^{-1,2} &= 145 \pm 97, \end{aligned} \right\} \quad (29)$$

with  $\epsilon = 1.096$ . These results were then used with the results for eccentricity in a SIMRES fitting (§5.4.4).

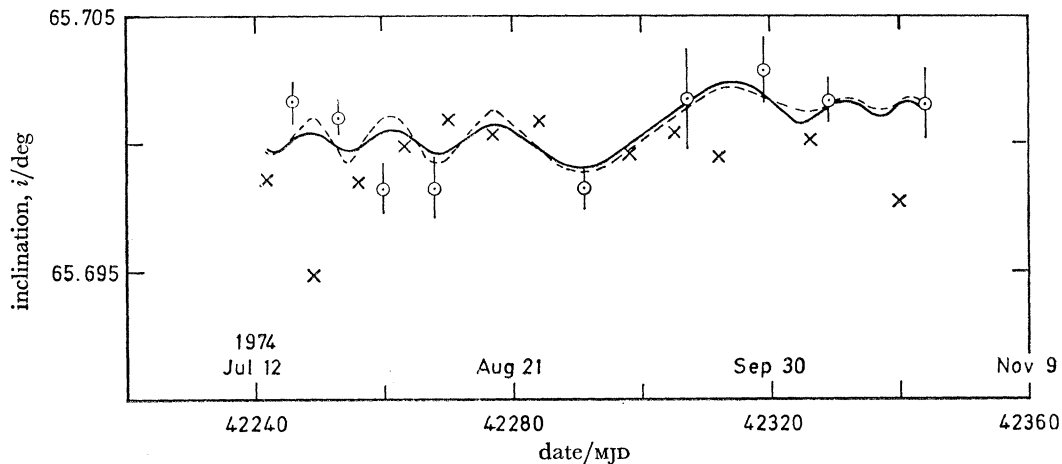


FIGURE 9. Variation of inclination at 15th-order resonance.  $\odot$ , from R.A.E. orbits;  $\times$ , from U.S. Navy orbits. —, THROE fitting of  $i$  alone; ----, SIMRES fitting of  $i$  and  $e$  together.

#### 5.4.3. Analysis of eccentricity, $e$

The same 21 orbits used in analysing the inclination were analysed to determine the effect of 15 : 1 resonance on the eccentricity: the U.S. Navy value at MJD 42333 was dropped again because it was inaccurate. All the 21 values of  $e$  were cleared of lunisolar and zonal harmonic perturbations with the aid of PROD. The PROD values were given the standard deviations quoted in table 2 and the U.S. Navy values were given standard deviations of 0.00008. The density scale height was taken as 35.5 km.

After the first THROE fitting with equation (27) it was again apparent that the U.S. Navy values suffered a bias relative to the PROD values (see §5.2.3). To overcome this bias, the quantity  $0.0002 \sin \omega$  was subtracted from each U.S. Navy value of eccentricity. In order to obtain the right adjustment for the effects of atmospheric drag by THROE, the values of  $M_2$  were changed using the technique described in §5.3.3.

After the first fitting with THROE, with  $(\gamma, q) = (1, 0)$ ,  $(1, 1)$  and  $(1, -1)$ , it was apparent that seven coefficients could not be determined from 21 values of eccentricity. As the  $(1, 0)$  terms have very little effect on eccentricity, the values were next fitted with  $(\gamma, q) = (1, 1)$  and  $(1, -1)$ . The values of the lumped coefficients obtained were

$$\left. \begin{aligned} 10^9 \bar{C}_{15}^{1,0} &= 124 \pm 64, & 10^9 \bar{S}_{15}^{1,0} &= 28 \pm 104, \\ 10^9 \bar{C}_{15}^{-1,2} &= -154 \pm 89, & 10^9 \bar{S}_{15}^{-1,2} &= -6 \pm 54, \end{aligned} \right\} \quad (30)$$

with  $\epsilon = 1.469$ . The fitted curve is shown as a full line in figure 10. The values of all the coefficients in equation (30) agree with those from equation (29) to within 1.3 times the sum of their standard deviations. So the prospect of achieving a better fit with SIMRES is good.

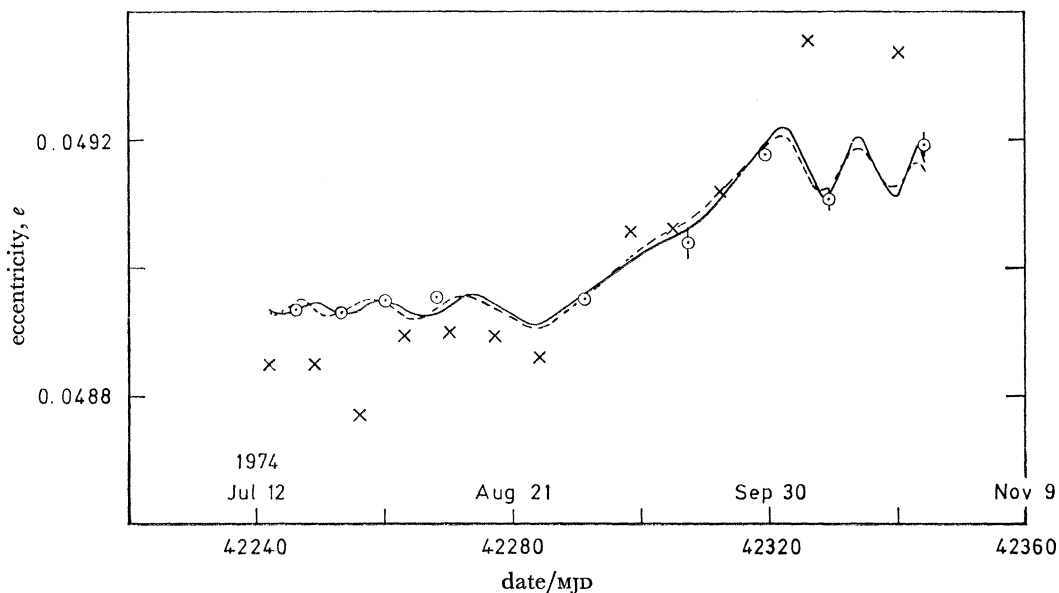


FIGURE 10. Variation of eccentricity at 15th-order resonance.  $\odot$ , from R.A.E. orbits;  $\times$ , from U.S. Navy orbits. —, THROE fitting of  $e$  alone; ----, SIMRES fitting of  $i$  and  $e$  together.

#### 5.4.4. Inclination and eccentricity fitted simultaneously

The values of inclination and eccentricity fitted separately by THROE with  $(\gamma, q) = (1, 1)$  and  $(1, -1)$  were next fitted simultaneously with the aid of the computer program SIMRES. As explained in §5.2.4, this program allows a choice of weighting. In the first fitting,  $i$  and  $e$  were given equal weight and in the second  $e$  was degraded by a factor equal to the ratio of the final values of  $\epsilon$  on the THROE fittings, namely  $1.340 (= 1.469/1.096)$ . The second fitting is the more logical, and gave lower standard deviations for all four lumped coefficients; so it was preferred. The fittings are shown in figures 9 and 10 by broken lines, and it is very satisfactory that these are just as good as the separate fittings (unbroken lines). The values of the lumped coefficients given by SIMRES are

$$\left. \begin{aligned} 10^9 \bar{C}_{15}^{1,0} &= 51 \pm 24, & 10^9 \bar{S}_{15}^{1,0} &= -55 \pm 7, \\ 10^9 \bar{C}_{15}^{-1,2} &= -67 \pm 10, & 10^9 \bar{S}_{15}^{-1,2} &= -19 \pm 24. \end{aligned} \right\} \quad (31)$$

It can be seen that the standard deviations here are much lower than those in equations (29) and (30), so the combined fitting is well worth-while. The values in equations (31) differ from the corresponding values in equations (29) by less than 1.7 times the sum of the standard deviations and from the corresponding values in equations (30) by less than 0.9 times the sum of the standard deviations. The individual differences for each coefficient expressed as multiples of the sum of the standard deviations are as follows:

	$\bar{C}_{15}^{1,0}$	$\bar{S}_{15}^{1,0}$	$\bar{C}_{15}^{-1,2}$	$\bar{S}_{15}^{-1,2}$
$i$	0.2	1.7	1.4	1.4
$e$	0.8	0.7	0.9	0.2.

The lumped coefficients in equations (31) should be useful in a future determination of the individual coefficients of the 15th order and even degree. In a previous determination (King-Hele *et al.* 1975*a*) there were no reliable values for inclinations near 65°.

## 6. ATMOSPHERIC ROTATION

### 6.1. Introduction

The upper atmosphere is rotating at approximately the same rate as the Earth: therefore the aerodynamic force acting on a satellite has a component perpendicular to the orbit, and this has the effect of reducing the inclination,  $i$ , of the orbit during the course of the satellite's life. For a high-drag satellite, atmospheric rotation is the most important force perturbing  $i$ ; so if the change in  $i$  is accurately measured, and other perturbations are removed, the rotation rate of the upper atmosphere in the region near the satellite's perigee can be determined, i.e. the zonal (west-to-east) wind speed near perigee can be evaluated.

The perturbations to be removed are caused by (1) lunisolar gravitational attraction, (2) zonal harmonics in the geopotential, (3) the  $J_{2,2}$  tesseral harmonic, (4) any change in  $i$  due to resonance and (5) the change in inclination due to meridional winds. The values of inclination are cleared of the effects of (1) and (2) by using the computer program PROD with one-day integration steps. The effect of perturbation (3) is removed by calculation of its numerical value for each PROP orbit. The resonances have already been analysed in §5, and the effects of meridional winds and other perturbations are discussed in §6.3.

### 6.2. Theory

The change  $\Delta i$  in the inclination of a satellite's orbit due to atmospheric rotation is given in terms of the change  $\Delta T_d$  in the satellite's orbital period, due to drag, by the equation (King-Hele & Scott 1966)

$$\begin{aligned} & \left[ 6F^{\frac{1}{2}} \left\{ 1 + 2e\frac{I_1}{I_0} + \frac{3}{4}e^2 \left( 1 + \frac{I_2}{I_0} \right) + c \left( \frac{I_2}{I_0} + 2e\frac{I_3}{I_0} \right) \cos(2\omega) \right\} \right] \frac{\Delta i}{\Delta T_d} \\ &= A \sin i \left[ 1 + \frac{I_2}{I_0} (1 + c) \cos(2\omega) - 2e\frac{I_1}{I_0} (1 + \cos(2\omega)) + \frac{1}{2}c \left( 1 + \frac{I_4}{I_0} \cos(4\omega) \right) \right. \\ &\quad \left. - ce \left\{ (1 + \cos(2\omega)) \frac{I_1}{I_0} + \frac{I_3}{I_0} \cos(2\omega) \right\} + e^2 \left\{ \left( \frac{3}{4} + \frac{1}{8} \cos(2\omega) \right) \right. \right. \\ &\quad \left. \left. + \frac{1}{4} (1 - \cos(2\omega)) \frac{I_2}{I_0} \right\} + O(c^3, e^3) \right]. \end{aligned} \quad (32)$$

In equation (32), which applies for an eccentricity of 0.2 or less,  $A$  is the angular velocity of the atmosphere (about the Earth's axis) in the region near perigee, divided by the Earth's angular velocity: thus  $A$  is strictly non-dimensional, but can conveniently be expressed in rev/day because the Earth's rotation rate is 1.0 rev/day. In equation (32) the change in orbital period  $\Delta T_d$  is expressed as a fraction of a day; the term in  $\cos(4\omega)$ , which was neglected in King-Hele & Scott (1966), has been restored.

Other parameters in equation (32) are as follows: the  $I_n$  are the Bessel functions of the first kind and imaginary argument, of degree  $n$  and argument  $z = ae/H$ , where  $H$  is the atmospheric density scale height. The parameter  $c$  takes account of atmospheric oblateness and is given by  $c = \{\epsilon' a(1 - e) \sin^2 i\} / 2H$ , where  $\epsilon'$  is the ellipticity of the atmosphere, taken the same as that of the



Earth, 0.00335. The factor  $F$  is given by  $\sqrt{F} = 1 - \{a(1-e)w \cos i\}/V_p$ , where  $V_p$  is the satellite's velocity at perigee and  $w$  is the angular velocity of the atmosphere near perigee. Usually  $\sqrt{F}$  has a value between 0.95 and 1.05. For 1971-106A, at inclination 65.7° with perigee height near 200 km,  $\sqrt{F} \approx 1 - 0.0025A$ .

The change in inclination due to meridional winds is given by (King-Hele 1966)

$$\frac{\Delta i}{\Delta T_d} = -\frac{\mu}{3\sqrt{F}} \cos i \left\{ \frac{2}{1 + \cos^2 i} \right\}^{\frac{1}{2}} \left\{ \left( 1 - \frac{K}{4} \right) \frac{I_1}{I_0} \cos \omega - \frac{KI_3}{4I_0} \cos(3\omega) + 0(0.1, e) \right\}, \quad (33)$$

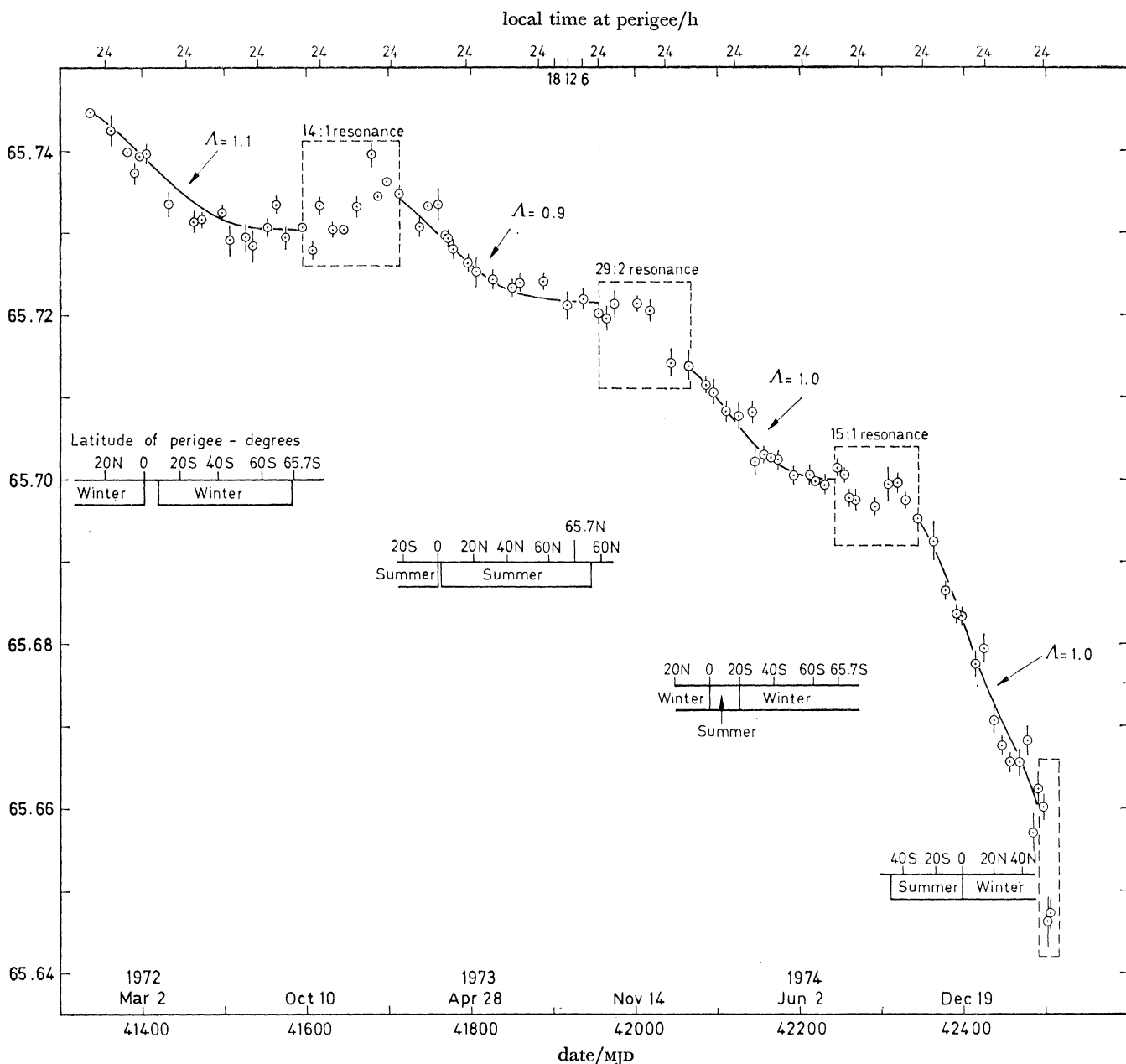


FIGURE 11. Values of inclination cleared of perturbations. The fittings to the points inside the boxes are shown in figures 5, 7, 9 and 12.

where  $K = \sin^2 i / (1 + \cos^2 i)$  and  $\mu$  is the south-to-north atmospheric rotation rate, that is the south-to-north wind speed (m/s) divided by  $rw_E$  where  $r$  is the distance from the Earth's centre (m) and  $w_E$  is the angular velocity of the Earth ( $72.7 \times 10^{-6}$  rad/s); so  $rw_E = 6580000 \times 72.7 \times 10^{-6} = 478$  m/s if perigee height is near 200 km.

### 6.3. Fitting of theoretical curves to the inclination

The values of orbital inclination from the 85 orbits of table 2 and the 15 orbits of table 4 have been cleared of the effects of lunisolar, zonal harmonic and  $J_{2,2}$  tesseral harmonic perturbations, and the values have been plotted as circles in figures 11 and 12. The 15 values of figure 12 can be regarded as superseding the last three values of figure 11.

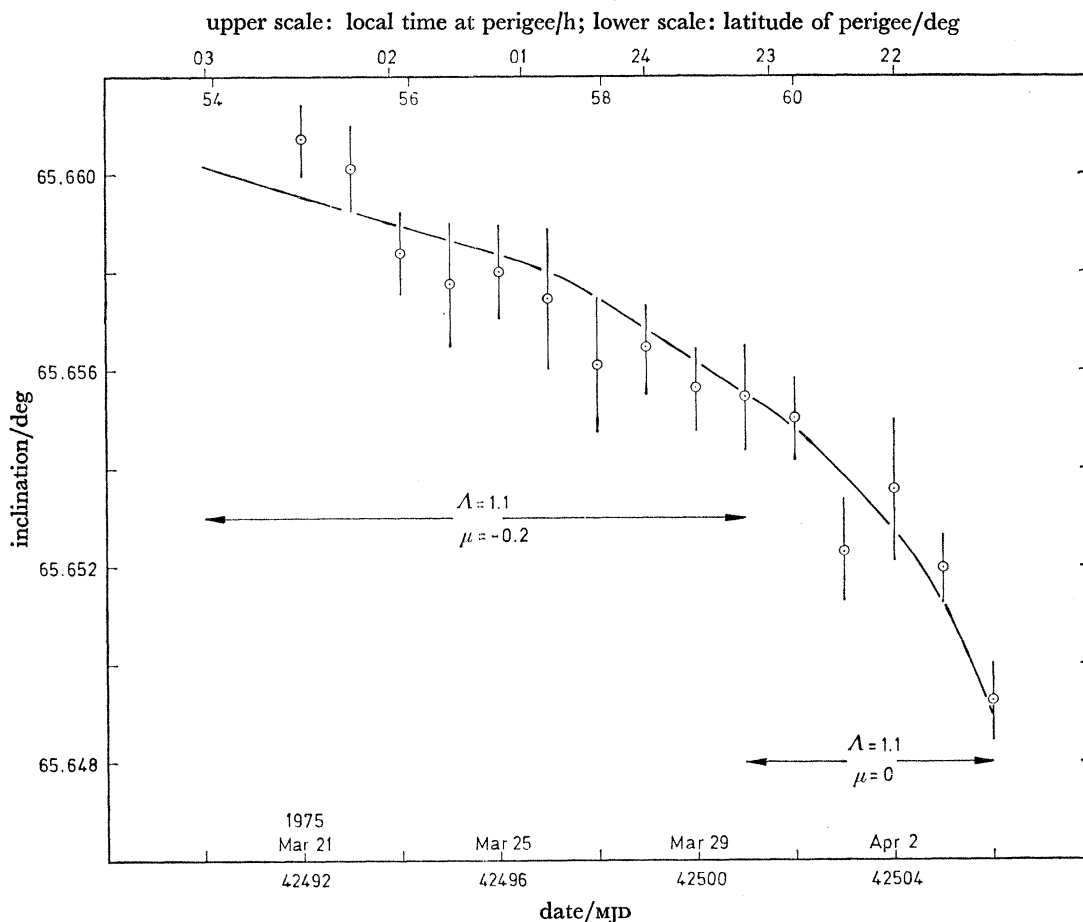


FIGURE 12. Values of inclination, cleared of perturbations, for last 15 days.

Perturbations in inclination due to Earth and ocean tides and solar radiation pressure have not been taken into account. The tidal perturbation in  $i$  for Geos 1, a satellite with an orbital inclination similar to 1971-106A, amounts to  $\pm 0.0004^\circ$  (Felsentreger *et al.* 1976). To allow for the neglect of this effect, all the standard deviations less than  $0.0005^\circ$  have been increased to  $0.0005^\circ$ . The effect of solar radiation pressure is very small: its effect on Explorer 24, a satellite in a comparable orbit but of much higher area-to-mass ratio, analysed by Slowey (1975), shows that the effect of solar radiation pressure on  $i$  for Cosmos 462 is likely to be of order  $0.00001^\circ$ .

The theoretical variation of  $i$  due to atmospheric rotation and meridional winds can be determined for a series of values of  $\Lambda$  and  $\mu$ , by using a computer program (ROTATM) based on equations (32) and (33). The theoretical variation of  $i$  was calculated for values of  $\Lambda$  between 0.8 and 1.4 at intervals of 0.1, with  $\mu = 0$  and 0.2, every 20 days throughout the satellite's life until the last 15 days, when the variation of  $i$  was evaluated daily. The values of  $i$  in figures 11 and 12 were then fitted with the best theoretical curves. Figure 11 divides naturally into four sections separated by the perturbations in inclination at 14:1, 29:2 and 15:1 resonances. These resonances have been analysed in §5 and the change in inclination due to resonance is available for each resonance. At the end of each resonance period the curve for atmospheric rotation is started at the value of  $i$  given at the end of resonance in the resonance analysis (see figures 5, 7 and 9), with atmospheric rotation perturbations restored. There is a fifth section to be fitted with a theoretical curve, for the last 15 days when the daily orbits are available (figure 12).

The variations in  $i$  due to meridional rotation, south-to-north winds, are proportional to  $\cos \omega$  (see equation (33)) and therefore the effect usually cancels out over one cycle of  $\omega$  for a fixed value of  $\mu$ . However, the value of  $\mu$  itself varies and both theoretical studies (Blum & Harris 1972, 1975; Ching & Straus 1977) and experimental results (Amayenc 1974; Blum & Harris 1975; Antoniadis 1976; Harper 1977) suggest that  $\mu$  has an approximately sinusoidal variation during the course of 24 h; with maximum wind towards the equator at about 02 h local time and maximum wind away from the equator at about 14 h. For 1971–106A the variation in  $\omega$  is slow (one cycle in about 1.8 years, see figure 3) and the local-time variations, indicated at the top of figure 11, are much faster, one cycle every 90 days approximately. The first four sections in figure 11 are all averaged in local time, covering about 200 days. The effect of  $\mu$  will therefore tend to cancel out, and the fittings were made with the  $\mu = 0$  curves. It is possible that the mean value of  $\mu$  is non-zero, but the effect is generally small: on the first section, for example, the effect of  $\mu = 0.05$  throughout would be to change  $i$  by  $0.0005^\circ$ .

So the values of inclination are fitted by choosing the best values of  $\Lambda$  assuming  $\mu = 0$  on the first four sections. After allowance has been made for the breaks at resonance, the best fit between theory and observations for the four sections of figure 11 was obtained with values of atmospheric rotation  $\Lambda$  of 1.1, 0.9, 1.0 and 1.0 respectively.

In order to assess the likely errors in these values of  $\Lambda$ , a realistic estimate of the likely errors in  $i$  at the beginning ( $i_b$ ) and end ( $i_e$ ) of each section,  $\sigma_b$  and  $\sigma_e$ , was made, and then the standard deviation in  $\Lambda$  was taken as  $\Lambda(\sigma_b^2 + \sigma_e^2)^{1/2} (i_b - i_e)^{-1}$ . For the first three sections of the curve in figure 11 the errors  $\sigma_b$  and  $\sigma_e$  are estimated as being between  $0.0005^\circ$  and  $0.0007^\circ$ , and this gives errors in  $\Lambda$  of near 0.05 on all three sections. For the fourth section the error in  $\Lambda$  is 0.02 on the same basis. This value is so small that other errors, hitherto neglected, may become significant: there is a possible error of about 0.01 from the neglect of  $O(\epsilon^3)$  terms in equation (32), and possibly errors approaching 0.01 from errors in the assumed atmospheric ellipticity. There may also be a small error, not more than 0.02, from neglect of the effects of 31:2 resonance.

There is a possibility that the atmospheric winds depend on season, so the latitude and 'seasonal bias' of perigee are indicated below the curve in figure 11.

In fitting the values of inclination in the last 15 days of the life (figure 12) the effect of meridional winds should be included. The season is near equinox and the perigee latitude is  $54\text{--}62^\circ\text{N}$ : in these conditions, the prevailing winds are (Blum & Harris 1972, 1975; Amayenc 1974; Antoniadis 1976; Harper 1977; Ching & Straus 1977) from north to south of order 100 m/s at local times from 23 h through midnight to 05 h, with only very weak winds from 17 to 23 h local time. So it is

appropriate in figure 12 to take  $\mu = -0.2$  up to March 30, and  $\mu = 0$  thereafter. With these values of  $\mu$ , the best fit is obtained with  $\Lambda = 1.1$ : the curve fits all the 15 values in figure 12 to within 1.5 s.d., and, taking  $\sigma_b$  and  $\sigma_e$  as slightly less than  $0.001^\circ$ , the s.d. in  $\Lambda$  is assessed as 0.1.

#### 6.4. Results

Previous studies of upper-atmosphere zonal winds (King-Hele & Walker 1977) have shown that the value of  $\Lambda$  varies with both height and local time. Figure 13 of King-Hele & Walker (1977) gives three curves for the variation of  $\Lambda$  with height, for evening (18–24 h), morning (04–12 h) and average values of local time. A revised version of this diagram is given as figure 2 of Walker (1978*b*).

TABLE 5. VALUES OF ATMOSPHERIC ROTATION RATE,  $\Lambda$ , OBTAINED FROM 1971–106A

date	height km	local time	'seasonal bias'	$\Lambda$
21 Jan.–2 Oct. 1972	253	average	winter	$1.1 \pm 0.05$
30 Jan.–30 Sept. 1973	250	average	summer	$0.9 \pm 0.05$
20 Jan.–14 July 1974	239	average	average	$1.0 \pm 0.05$
24 Oct. 1974–19 Mar. 1975	218	average	average	$1.0 \pm 0.03$
19 Mar.–4 Apr. 1975	199	03–21 h	—	$1.1 \pm 0.1$

The results obtained here are listed in table 5. The values of  $\Lambda$  are given for each section of figure 11 and for figure 12, together with an estimate of the height and local time at which the values apply. The 'seasonal bias', as given by the latitude of perigee and time of year (see figure 11), is also indicated. The height is taken as  $\frac{3}{4}H$  above the average perigee height (King-Hele & Scott 1969).

The first section of the fitted curve in figure 11 gives a value of  $\Lambda = 1.1$ , and during nearly the whole of this period the perigee is experiencing 'winter' conditions. For the second section, with  $\Lambda = 0.9$ , the perigee is enjoying predominantly 'summer' conditions; for the third and fourth sections, where  $\Lambda = 1.0$ , perigee has average seasonal conditions. (Although the third section may seem to have a bias towards 'winter' the short 'summer' occurs during the time of greatest change in  $i$ .) These results suggest that  $\Lambda$  may be higher in winter than in summer. Such a seasonal dependence of  $\Lambda$  has not been detected before in the analysis of satellite orbits, but measurements at specific sites by the radar back-scatter method (Antoniadis 1976; Hernandez & Roble 1976; Roble, *et al.* 1977) indicate that the strongest west-to-east winds usually occur in the winter, i.e.  $\Lambda$  is higher in the winter. The results here lend support to this conclusion.

The first four values of  $\Lambda$  in table 5 (for average local time) are all below the average curve in figure 2 of Walker (1978*b*). This decrease in the value of  $\Lambda$  can also be detected in other analyses of satellite orbits (Walker 1974; Hiller 1975, 1978) between 1971 and 1976, when compared with the average curve of Walker (1978*b*) which is based mainly on results from the 1960s. So it seems possible that the average rotation rate of the upper atmosphere has decreased during the early 1970s: further evaluations of atmospheric rotation rate are needed before this tentative conclusion can be confirmed.

The value obtained for the last 15 days in orbit,  $\Lambda = 1.1 \pm 0.1$  at a height of 199 km, is at a time close to equinox, but it is not averaged over all local times like the other values. The local time runs from 03 h through midnight to 21 h and there is a mild bias towards the evening hours because the decrease in inclination is then more rapid. So the value might be described as

'average with a slight bias towards evening', and indicates west-to-east winds of  $25 \pm 25$  m/s at an average latitude of  $58^\circ$  N. Results for such high latitudes are unusual in satellite orbital analysis, because the effect of atmospheric rotation becomes very small as perigee approaches apex (maximum latitude) and it is not usually possible to obtain accurate values of  $A$ . The successful results obtained here are attributable to (a) the large change in orbital period in the last few days before decay, and (b) the frequent and accurate orbits obtained with the aid of the NORAD observations.

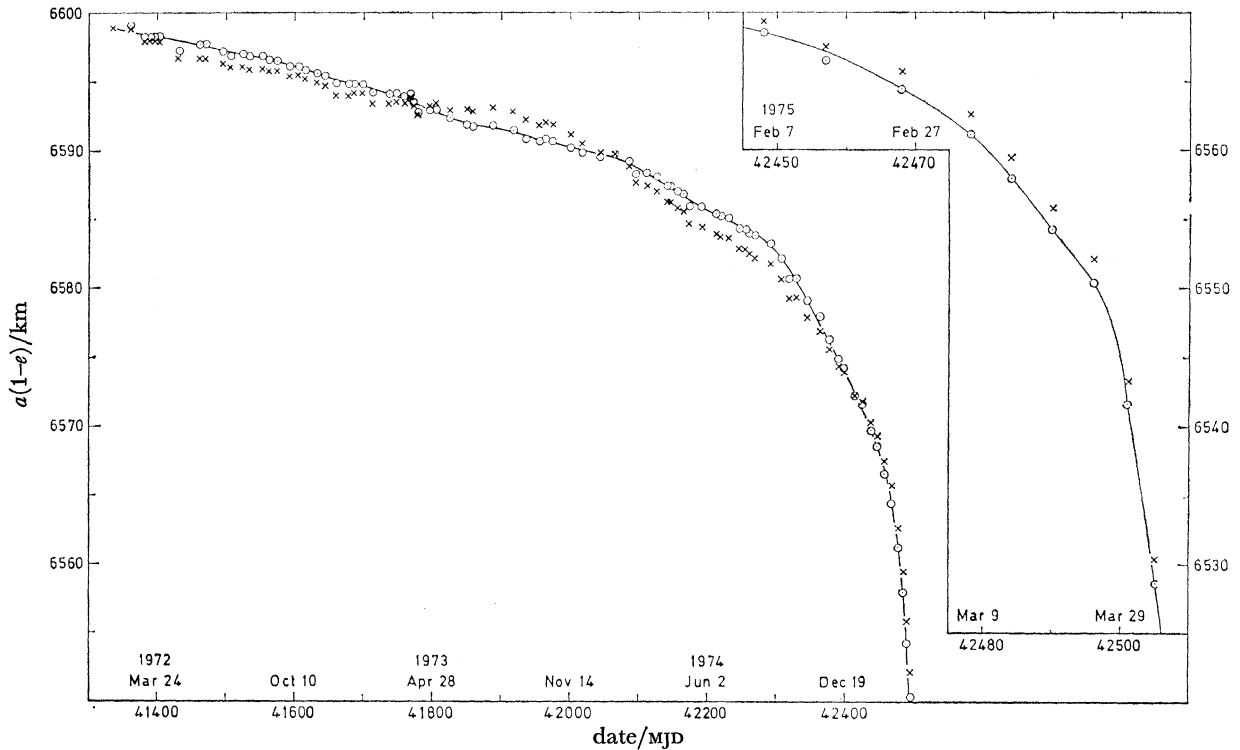


FIGURE 13. Values of  $a(1-e)$ .  $\times$ , from the 85 orbits;  $\circ$ , after removal of perturbations; —, smooth curve through  $\circ$  values.

## 7. DENSITY SCALE HEIGHT

### 7.1. Introduction

The perigee distance,  $a(1-e)$ , gradually decreases under the influence of air drag, and the decrease is proportional to the density scale height,  $H$ . So values of  $H$  can be found from the decrease in  $a(1-e)$ . If the odd zonal harmonic and lunisolar perturbations are removed from  $a(1-e)$ , by using PROD, the remaining variation should show a steady decrease as a result of air drag alone. Figure 13 shows the values of  $a(1-e)$  from table 2 as crosses; the values after removal of perturbations,  $Q$ , are plotted as circles, with a smooth curve drawn through the points. Figure 14 is a similar diagram for the 15 daily orbits (table 4) before decay. The curve of figure 14 can be regarded as superseding that of figure 13 from MJD 42 492 onwards. The variation of  $Q$ , in figures 13 and 14, shows a fairly smooth decrease due to the action of air drag.

## 7.2. Method

The theoretical equation for the variation of  $Q$  is (King-Hele & Walker 1971)

$$\dot{Q} = -\frac{2H_1 M_2}{3M_1 e} \left\{ 1 - 2e + \frac{H_1}{4ae} - \frac{2e'}{e} \sin^2 i \cos(2\omega) + O\left(e^2, \frac{H}{a}, \frac{H^2}{a^2 e^2}, \frac{e'^2}{e^2}\right) \right\}, \quad (34)$$

where  $H$  is the density scale height,  $H_p$  is the value of  $H$  at perigee,  $H_1$  is the value of  $H$  at a height  $1.5 H_p$  above perigee, and  $e'$  is the ellipticity of the atmosphere, taken as equal to the Earth's ellipticity, 0.00335. Equation (34) is valid for  $ae/H_p > 3$ .

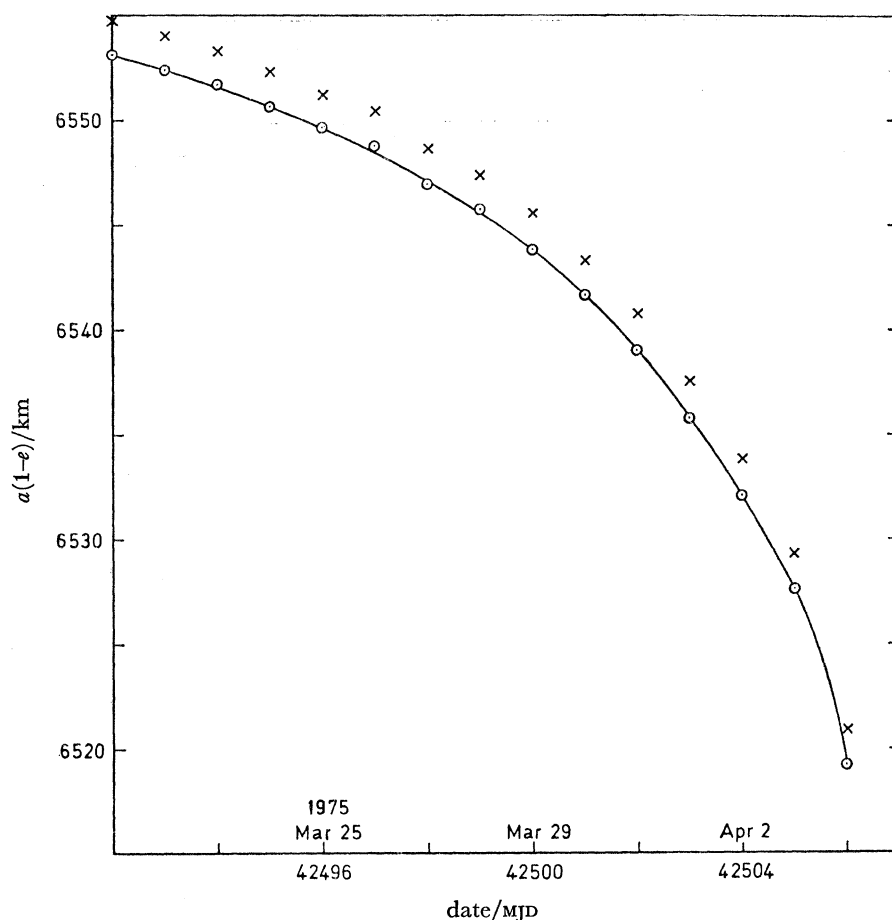


FIGURE 14. Variation of  $a(1-e)$  for last 15 days.  $\times$ , from the 15 orbits of table 4;  $\circ$ , after removal of perturbations; —, smooth curve through  $\circ$  values.

Average values of  $\dot{Q}$  were calculated over a time-interval,  $\Delta t$ , long enough to ensure that an accurately measurable change,  $\Delta Q$ , in  $Q$ , has occurred. The values of  $\Delta Q/\Delta t$  serve as values of  $\dot{Q}$  in equation (34), and averaged values of  $M_1$ ,  $M_2$ ,  $e$ ,  $a$ ,  $i$  and  $\cos(2\omega)$  over the corresponding  $\Delta t$  were used to calculate values of  $H_1$  from equation (34).

For 1971-106A, the value of  $ae/H_p$  exceeds 3 from launch until mjd 42495, and 17 values of  $H_1$  were calculated during this time: they are plotted as circles in figure 15, and the time over which they are averaged is indicated. The corresponding average values of height  $y_1 (= y_p + 1.5 H_p)$  are given at the top of figure 15. The standard deviations in the values of  $H_1$  derive from the estimated

errors in the values of  $\Delta Q$  arising from errors in  $Q$ . The errors due to neglected terms in (34) are smaller than the errors in  $\Delta Q$ , and are ignored.

After MJD 42495, when the value of  $ae/H_p$  falls below 3, equation (34) becomes inaccurate, and the small-eccentricity form of the theory must be used. The theoretical equation for  $H_1$  when  $ae/H_p < 3$  is  $H_1 = \Delta Q/f(z)$ , where  $z = ae/H_1$  and

$$f(z) = \{(r_{p1} - r_p)/H\}_{\text{sph. atm.}} - \{\psi(z) - \psi(z_1)\}. \quad (35)$$

Values of  $(r_{p1} - r_p)/H$  for a spherical atmosphere are given in figure 18 of King-Hele *et al.* (1960); and  $\{\psi(z) - \psi(z_1)\}$ , the oblateness correction, is given in figure 22 of King-Hele *et al.*

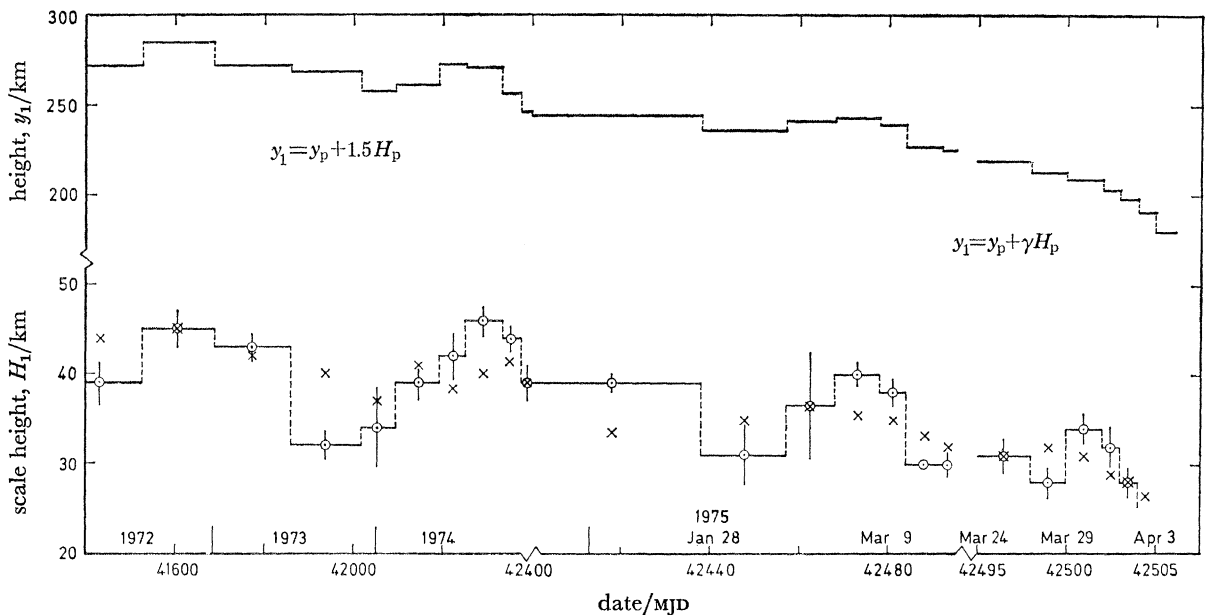


FIGURE 15. Values of density scale height  $H_1$  at height  $y_1$  for 1972-5.  $\circ$ , Values of scale height derived from decrease in  $Q$ , with s.d.  $\times$ , Values of scale height from CIRA (1972).

(1960). The values of  $H_1$  apply at a height  $\gamma H_p$  above perigee, where  $\gamma$  is given in figure 9 of King-Hele & Cook (1962). Seven values of  $H_1$  were evaluated between MJD 42495 and decay, the last four being daily values. For these seven values, the observed values of  $e$  must be corrected for the odd-harmonic oscillation, and this was done with the aid of PROD. These seven values of  $H_1$  are also plotted as circles in figure 15 with their standard deviations. The s.d. is the estimated error in the value of  $\Delta Q$  (between 1.2% and 3.8%) arising from errors in  $Q$ , together with the estimated error in reading figures 18 and 22 of King-Hele *et al.* (1960) (between 2% and 6%). The errors due to neglected terms in equation (35) should be less than 1%, and are ignored. The corresponding average values of height  $y_1 (= y_p + \gamma H_p)$  are given at the top of figure 15.

The values of  $H_1$  plotted as crosses in figure 15 are the values of density scale height obtained from the COSPAR International Reference Atmosphere 1972 (CIRA 1972) for heights  $y_1$  and the appropriate exospheric temperatures,  $T_\infty$ , obtained from Walker (1978a).

### 7.3. Discussion of results

The general impression gained from studying figure 15 is that the CIRA 1972 values are in fairly good agreement with the values from the orbital analysis. This confirms the accepted

opinion that CIRA 1972 represents the scale height  $H$ , a very variable parameter, fairly accurately. The average difference between the observational and CIRA 1972 values in figure 15 is about 1%, while the r.m.s. difference is about 10%.

Three of the observational values in figure 15 differ from the CIRA values by more than 5 km, those at MJD 41 859–42 018 (1973 June 26–December 2), MJD 42 253–42 329 (1974 July 25–October 9) and MJD 42 398–42 438 (1974 December 17–1975 January 26).

The first of these values is low compared with that given by CIRA, probably because the density is low over this period, relative to other years (see figure 14 of Walker 1978*a*). The second value, which is higher than CIRA, is at a time when density is fairly average (see figure 14 of Walker 1978*a*), although it is rising towards the end of the period, so no reason for this high value can be given. The third value, from 1974 December 17 to 1975 January 26, which is also higher than CIRA, is however explained by the above-average values of density over the whole period (see figure 8 of Walker 1978*a*).

The results also show that it is possible to obtain accurate and consistent daily values of  $H$  at the end of the satellite's life when good orbits are available from numerous observations. These last few values are also in good agreement with CIRA 1972.

## 8. CONCLUSIONS

The orbit of 1971–106A has been determined at 85 epochs during its 40-month life from 6635 observations. The accurate Hewitt camera observations were used in 24 of these orbits, in which the average s.d. in inclination corresponds to about 80 m in distance; while for the other 61 orbits the average s.d. corresponds to about 170 m in distance. The other orbital parameters show improved accuracy with the camera observations, but to a lesser degree. The residuals of the observations have been sent to the observers.

A further 2000 observations were received from NORAD covering the last 15 days of the satellite's life. With these observations, 15 daily orbits were determined. These orbits at the end of the satellite's life are more accurate and at closer intervals than has been possible in the past; the average s.d. in inclination corresponds to about 120 m in distance.

Analysis of the inclination and eccentricity at 14:1, 29:2 and 15:1 resonances, has yielded lumped values of the harmonic coefficients of order 14, 29 and 15. The lumped 14th-order coefficients from fitting  $i$  and  $e$  with SIMRES are given in equation (16) and have been used in a recent evaluation of the 14th order-harmonics. The analysis of the change in inclination at 29:2 resonance yielded lumped coefficients, equation (22), which should be useful in the future in determining the individual coefficients of order 29. The variation in eccentricity was too small to analyse successfully. The SIMRES fitting of inclination and eccentricity at 15th-order resonance was very satisfactory. The lumped coefficients are given in equation (31) and will be useful in a further determination of the individual coefficients of 15th order.

The variation of inclination between the resonances has been analysed to obtain four values of the average atmospheric rotation rate,  $A$ . The results are summarized in table 5. Because of the very slow movement of perigee, two of the values of  $A$  had strong seasonal bias and the results suggest that  $A$  may be higher in winter than in summer. This seasonal difference has not been detected before from analysis of satellite orbits, but is in agreement with measurements at specific sites by the radar back-scatter method. The values of  $A$  are lower than expected, and it seems possible that the average rotation rate of the upper atmosphere was lower during the early



1970s than in the 1960s. The daily orbits over the last 15 days of the satellite's life give west-to-east winds of  $25 \pm 25$  m/s at an average latitude of  $58^\circ$  N. Results for such high latitude are unusual, but are possible here due to the large change in orbital period in the last few days before decay, and the frequent and accurate orbits obtained with the aid of NORAD observations.

Values of density scale height,  $H_1$  have been determined from analysis of the variation of perigee height. A total of 24 values was obtained during the satellite's 40 month life: eight of these were in the last 15 days of the life and the last four were daily. The values obtained show fairly good agreement with CIRA 1972; the average difference between the observational and CIRA 1972 values is about 1% and the r.m.s. difference 10%. Only three observational values differ from CIRA 1972 by more than 5 km and reasons for two of these differences have been suggested. The agreement shows that CIRA 1972 provides a good measure of the density scale height for the years 1972–5.

## REFERENCES

- Allan, R. R. 1973 *Planet. Space Sci.* **21**, 205–225.
- Amayenc, P. 1974 *Radio Sci.* **9**, 281–293.
- Antoniadis, D. A. 1976 *J. atmos. terr. Phys.* **38**, 187–195.
- Blum, P. W. & Harris, I. 1972 *Space Research XIII*, pp. 369–375. Berlin: Akademie Verlag.
- Blum, P. W. & Harris, I. 1975 *J. atmos. terr. Phys.* **37**, 213–235.
- Ching, B. K. & Straus, J. M. 1977 *J. atmos. terr. Phys.* **39**, 1389–1394.
- CIRA 1972 *Cospar international reference atmosphere 1972*. Berlin: Akademie Verlag.
- Cook, G. E. 1973 *Celest. Mech.* **7**, 301–314.
- Felsentreger, T. L., Marsh, J. G. & Agreen, R. W. 1976 *J. geophys. Res.* **81**, 2557–2563.
- Freedman, L. 1977 *Survival*, **19**, No. 1, 16–23.
- Gooding, R. H. 1971 *Tech. Repts R. Aircr. Establ.* **71068**.
- Gooding, R. H. 1974 *Tech. Repts R. Aircr. Establ.* **74164**.
- Gooding, R. H. 1979 Studies of resonance in the orbits of Ariel satellites. *Tech. Repts R. Aircr. Establ.* (to be issued).
- Gooding, R. H. & Tayler, R. J. 1968 *Tech. Repts R. Aircr. Establ.* **68299**.
- Harper, R. M. 1977 *J. geophys. Res.* **82**, 3243–3250.
- Hernandez, G. & Roble, R. G. 1976 *J. geophys. Res.* **81**, 2065–2074.
- Hiller, H. 1972 *Tech. Repts R. Aircr. Establ.* **72147**.
- Hiller, H. 1975 *Planet. Space Sci.* **23**, 1369–1376.
- Hiller, H. 1978 *Tech. Repts R. Aircr. Establ.* **78107**.
- Kaula, W. M. 1966 *Theory of satellite geodesy*. Waltham, Mass: Blaisdell.
- King-Hele, D. G. 1966 *Proc. R. Soc. Lond. A* **294**, 261–272.
- King-Hele, D. G. 1974 *Planet. Space Sci.* **22**, 509–524.
- King-Hele, D. G. & Cook, G. E. 1962 *Tech. Notes R. Aircr. Establ. Space* **18**.
- King-Hele, D. G. & Cook, G. E. 1974 *Planet. Space Sci.* **22**, 645–672.
- King-Hele, D. G., Cook, G. E. & Walker, D. M. C. 1960 *Tech. Notes R. Aircr. Establ. GW* **565**.
- King-Hele, D. G. & Scott, D. W. 1966 *Planet. Space Sci.* **14**, 1339–1365.
- King-Hele, D. G. & Scott, D. W. 1969 *Planet. Space Sci.* **17**, 217–232.
- King-Hele, D. G. & Walker, D. M. C. 1971 *Planet. Space Sci.* **19**, 1637–1651.
- King-Hele, D. G. & Walker, D. M. C. 1977 *Planet. Space Sci.* **25**, 313–336.
- King-Hele, D. G., Walker, D. M. C. & Gooding, R. H. 1975a *Planet Space Sci.* **23**, 229–246.
- King-Hele, D. G., Walker, D. M. C. & Gooding, R. H. 1975b *Planet. Space Sci.* **23**, 1239–1256.
- King-Hele, D. G., Walker, D. M. C. & Gooding, R. H. 1979 *Planet. Space Sci.* **27**, 1–18.
- Klokočnik, J. 1976 *Bull. astr. Insts Cz.* **27**, 287–295.
- Perry, G. E. 1977 *R.A.F.Q.* **17**, 328–335.
- Pilkington, J. A., King-Hele, D. G., Hiller, H. & Walker, D. M. C. 1979 *Tech. Repts R. Aircr. Establ.* **79001**.
- Roble, R. G., Salah, J. E. & Emery, B. A. 1977 *J. atmos. terr. Phys.* **39**, 503–511.
- Scott, D. W. 1969 *Tech. Repts R. Aircr. Establ.* **69163**.
- Sheldon, C. S. II 1976 *Soviet Space Programs, 1971–75*, vol. 1, pp. 424–429. Washington: U.S. Government Printing Office.
- Slowey, J. W. 1975 *Planet. Space Sci.* **23**, 879–886.
- Walker, D. M. C. 1974 *Planet. Space Sci.* **22**, 391–402.
- Walker, D. M. C. 1975 *Planet. Space Sci.* **23**, 565–574.
- Walker, D. M. C. 1977 *Planet. Space Sci.* **25**, 337–342.
- Walker, D. M. C. 1978a *Planet. Space Sci.* **26**, 291–309.
- Walker, D. M. C. 1978b *J. Br. interplanet. Soc.* **31**, 197–199.

TABLE 1. SOURCES OF THE OBSERVATIONS USED IN EACH RUN

run no.	source of observations						total
	Hewitt camera	Cape kinethe- odolite	visual	British radar	U.S. Navy	Finland	
1	10E	4	11		29		54
2		6	5		38		49
3	15M		41		31		87
4		4	35		47		86
5	5E, 4M	2	37	6	26		80
6	1M		39		15		55
7		2	20	15	39		76
8			28		30		58
9			46		25		71
10	5M		10		36		51
11			21		47		68
12			2		34		36
13			10		56		66
14			13		76		89
15			15	5	46		66
16			35		36		71
17	5E, 7M		43		40		95
18			35		34	29	98
19	4E		23		56	5	88
20		2	3		34		39
21	10E		14		53		77
22			15		35		50
23			43		45	3	91
24	10M		26	17	40	18	111
25	10E		7	38	29		84
26	5M		5	38	25		73
27			3	46	33		82
28	5M, 5E		9	50	32		101
29		12	18	36	24		90
30	15E, 15M	2	51	16	2	3	104
31	5M		41	12	18		76
32			26	44	18	16	104
33	5M		5	40	17		67
34			9	34	22		65
35		6	9	21	28		64
36	5M		17	20	22		64
37	6M	8	9	18	21		62
38	10M		3	46	33		92
39		14	14	30	18		76
40	5E		3	17	26		51
41		6	10	10	35		61
42			6	33	22		61
43			11	36	27	4	78
44		16	37	24	25	3	105
45		4	7	34	26		71
46		4	3	35	30		72
47		2	4	36	25		67
48	5M		32	30	31		98
49		8	39	40	31		118
50			4	48	41		93
51			7	44	32		83
52		4	6	28	23	3	64
53			44	24	16	9	93
54		2	16	36	28	12	94

TABLE 1 (*cont.*)

run no.	Source of observations						total
	Hewitt camera	Cape kinethe- odolite	visual	British radar	U.S. Navy	Finland	
55	5M		21	30	39	15	110
56			24	36	35		95
57				35	43		78
58			13	39	35		87
59	10M		13	36	36		95
60		2	13	50	32		97
61	5M		24	48	41		118
62	5M		12	36	24		77
63			48	42	34		124
64			9	54	32		95
65				31	33		64
66			4	42	27		73
67			10	44	33		87
68			25	50	33		108
69			11	40	34		85
70		2	10	48	31		91
71		2	3	58	30		93
72		6	6	44	23		79
73			13	42	28		83
74			4	44	29		77
75			4	52	17		73
76			2	56	18		76
77		4	5	66	25		100
78			2	52	20		74
79				56	21		77
80			4	50	17		71
81		2		36	24		62
82				34	10		44
83				28	17		45
84				8	13		21
85				41	10		51
total	197	126	1305	2335	2552	120	6635

E, observations made by Edinburgh Hewitt camera.

M, observations made by Malvern Hewitt camera.

## NOTATION IN TABLES 2 AND 4.

MJD	modified Julian day	$M_0$	mean anomaly at epoch (deg)
$a$	semi major axis (km)	$M_1$	mean motion $n$ (deg/day)
$e$	eccentricity	$M_2, M_3, M_4, M_5$	later coefficients in the polynomial for $M$
$i$	inclination (deg)	$\epsilon$	measure of fit
$\Omega$	right ascension of ascending node (deg)	$N$	number of observations used
$\omega$	argument of perigee (deg)	$D$	time covered by the observations (days)

TABLE 2. VALUES OF THE ORBITAL PARAMETERS AT 85 EPOCHS, WITH STANDARD DEVIATIONS

MJD	date	$a$	$e$	$i$	$\Omega$	$\omega$	$M_0$	$M_1$	$M_2$	$M_3$	$M_4$	$M_5$	$\epsilon$	$N$	$D$	$a(1-e)$
1*	41337	21 Jan. 1972	7374.904	0.105214	65.7435	176.133	30.84	321.45	4935.575	0.1963	0.00230	0.00052	0.90	45	9.1	6598.96
			1	7	4	1	1	1	1	5	7	2				
2	41362	15 Feb. 1972	7364.928	0.104027	65.7451	113.068	18.77	359.27	4945.609	0.2240	0.00233	-0.00016	0.99	44	9.4	6598.78
			1	10	18	2	1	1	1	3	5	2				
3*	41381	5 Mar. 1972	7354.598	0.102880	65.7390	64.926	9.57	101.08	4956.033	0.2939	0.00011	0.00066	0.76	70	7.5	6597.96
			1	8	1	<1	<1	<1	1	5	9	5				
4	41390	14 Mar. 1972	7348.950	0.102185	65.7375	42.039	5.23	90.74	4961.749	0.3286	0.00294	0.00037	0.68	78	9.9	6598.00
			<1	9	11	1	<1	<1	<1	3	3	1				
5*	41398	22 Mar. 1972	7343.143	0.101481	65.7429	21.646	1.34	207.83	4967.637	0.3788	0.00128	—	0.62	60	5.8	6597.95
			1	14	5	1	1	1	1	3	21	—				
6*	41404	28 Mar. 1972	7338.621	0.100938	65.7451	6.318	358.43	147.53	4972.231	0.3635	-0.00331	—	0.62	43	5.7	6597.88
			2	29	10	2	1	1	2	5	29	—				
7	41431	24 Apr. 1972	7322.282	0.099097	65.7332	297.007	345.20	347.63	4988.885	0.2602	-0.00425	-0.00013	0.74	61	9.1	6596.67
			1	15	15	2	1	1	1	5	7	3				
8	41462	25 May 1972	7308.221	0.097363	65.7338	216.890	329.98	68.14	5003.292	0.2162	-0.00143	—	0.53	50	7.4	6596.67
			1	15	13	1	1	1	1	2	13	—				
9	41471	3 June 1972	7304.608	0.096920	65.7310	193.543	325.54	114.57	5007.005	0.2143	0.00294	—	0.60	59	8.0	6596.65
			1	12	10	1	1	1	1	2	9	—				
10*	41498	30 June 1972	7292.025	0.095414	65.7332	123.235	312.14	120.08	5019.972	0.2124	-0.00290	—	0.47	47	5.0	6596.26
			1	12	8	1	1	1	1	5	31	—				
11	41507	9 July 1972	7288.338	0.094992	65.7319	99.715	307.66	316.58	5023.783	0.2232	-0.00222	-0.00028	0.81	62	8.7	6596.00
			2	18	20	2	1	1	2	6	14	4				
12	41526	28 July 1972	7281.857	0.094181	65.7293	49.948	298.18	74.60	5030.492	0.1576	-0.00154	—	0.49	30	4.9	6596.04
			2	12	17	1	1	1	2	9	42	—				
13	41534	5 Aug. 1972	7279.267	0.093876	65.7284	28.948	294.23	8.38	5033.178	0.2490	0.00215	-0.00273	0.78	49	7.1	6595.92
			2	12	19	2	1	1	2	12	22	10				
14	41552	23 Aug. 1972	7273.706	0.093184	65.7351	341.616	285.16	300.09	5038.953	0.1676	-0.00089	0.00020	0.42	70	9.7	6595.91
			1	7	10	1	1	1	1	3	18	1				
15	41562	2 Sept. 1972	7269.595	0.092708	65.7375	315.269	280.19	309.36	5043.228	0.2449	-0.00034	-0.00023	0.44	54	7.3	6595.65
			1	8	10	1	1	1	1	7	10	5				
16	41575	15 Sept. 1972	7263.646	0.091958	65.7293	280.941	273.66	31.20	5049.426	0.2684	-0.00403	-0.00152	0.55	61	5.3	6595.70
			1	10	13	1	1	1	1	13	31	20				
17*	41592	2 Oct. 1972	7255.616	0.090996	65.7293	235.906	265.10	262.13	5057.812	0.2180	-0.00119	0.00105	0.48	82	6.9	6595.38
			1	6	4	1	1	1	1	12	46	14				
18	41607	17 Oct. 1972	7249.712	0.090246	65.7299	196.055	257.49	215.31	5063.994	0.2015	0.00197	0.00190	0.47	80	5.0	6595.45
			2	9	10	1	1	1	2	19	38	26				
19*	41616	26 Oct. 1972	7245.167	0.089720	65.7336	172.088	252.93	91.87	5068.760	0.2817	0.00121	0.00039	0.52	77	7.5	6595.13
			1	10	8	1	1	1	1	5	10	4				
20	41631	10 Nov. 1972	7237.228	0.088756	65.7274	132.032	245.36	230.04	5077.104	0.2093	—	—	0.39	35	5.0	6594.88
			1	6	8	1	1	1	1	3	—	—				
21*	41644	23 Nov. 1972	7231.415	0.088070	65.7305	97.215	238.72	29.79	5083.228	0.2838	0.00295	—	0.56	67	7.5	6594.54
			1	2	2	<1	1	1	1	2	11	—				
22	41660	9 Dec. 1972	7222.561	0.087033	65.7366	54.227	230.58	77.81	5092.581	0.2740	—	—	0.48	45	7.1	6593.96
			<1	12	12	1	1	1	<1	2	—	—				

TABLE 2 (cont.)

MJD	date	$a$	$e$	$i$	$\Omega$	$\omega$	$M_0$	$M_1$	$M_2$	$M_3$	$M_4$	$M_5$	$\epsilon$	$N$	$D$	$a(1-e)$
23	41679	28 Dec. 1972	7 211.535	0.085637	65.7405	2.969	110.28	5 104.267	0.2293	-0.00075	—	—	0.64	68	6.9	6 593.96
			1	19	16	2	1	1	3	13						
24*	41686	4 Jan. 1973	7 208.839	0.083279	65.7350	3 44.020	217.24	5 107.130	0.1849	0.00794	-0.00049	—	0.54	90	5.3	6 594.08
			1	15	3	1	1	1	11	26						
25*	41699	17 Jan. 1973	7 203.370	0.084581	65.7398	308.787	210.54	5 112.950	0.1980	-0.00292	—	—	0.46	79	5.7	6 594.10
			1	11	3	1	<1	1	2	15						
26*	41712	30 Jan. 1973	7 197.766	0.083964	65.7372	273.468	203.81	5 118.923	0.2429	-0.00333	—	—	0.54	69	5.6	6 593.41
			1	18	7	1	1	1	4	23						
27	41739	26 Feb. 1973	7 181.911	0.081949	65.7294	199.766	189.78	5 135.886	0.3962	-0.00120	0.00028	—	0.62	76	7.7	6 593.36
			2	21	12	1	1	2	6	29						
28*	41749	8 Mar. 1973	7 174.605	0.080994	65.7353	172.330	184.62	5 143.735	0.3841	-0.00502	—	—	0.42	81	5.4	6 593.51
			<1	8	4	1	<1	<1	2	8						
29	41760	19 Mar. 1973	7 166.919	0.080019	65.7353	142.040	178.84	5 152.013	0.3901	0.01490	-0.00017	-0.00055	0.95	66	7.1	6 593.43
			3	15	19	1	1	3	12	81						
30*	41769	28 Mar. 1973	7 160.820	0.079180	65.7292	117.181	174.14	5 158.598	0.3092	-0.00228	—	—	0.72	91	4.0	6 593.83
			<1	15	2	<1	<1	<1	1	23						
31*	41772	31 Mar. 1973	7 159.221	0.079052	65.7277	108.880	172.55	5 160.325	0.2766	—	—	—	0.53	53	3.1	6 593.27
			2	20	9	2	1	2	11	—						
32	41779	7 Apr. 1973	7 154.727	0.078570	65.7261	89.483	168.88	5 165.190	0.3211	-0.00070	-0.00063	—	0.53	89	5.9	6 592.58
			1	18	10	2	1	1	10	23						
33*	41797	25 Apr. 1973	7 144.453	0.077165	65.7296	39.441	159.33	5 176.338	0.2782	0.00933	—	—	0.58	42	4.8	6 593.15
			2	18	10	1	1	2	6	44						
34	41806	4 May 1973	7 139.215	0.076454	65.7299	14.341	154.54	5 182.036	0.2811	0.00391	0.00386	-0.00137	0.79	45	5.3	6 593.39
			4	25	18	2	1	4	24	200						
35	41826	24 May 1973	7 128.206	0.075102	65.7251	318.348	143.90	5 194.048	0.3107	-0.00917	0.00030	0.00021	0.81	49	7.7	6 592.86
			2	13	11	1	1	2	9	65						
36*	41850	17 June 1973	7 115.575	0.073476	65.7266	250.798	131.03	5 207.887	0.2601	—	—	—	0.72	56	5.3	6 592.75
			1	16	9	2	1	1	3	—						
37*	41859	26 June 1973	7 111.572	0.072965	65.7255	225.368	126.24	5 212.285	0.2280	-0.01194	-0.00054	0.00044	0.74	52	7.7	6 592.68
			2	15	10	2	1	2	5	40						
38*	41889	26 July 1973	7 102.681	0.071750	65.7253	140.361	110.07	5 222.078	0.1704	0.00913	0.00134	—	0.72	55	6.2	6 593.06
			1	2	9	2	2	1	10	12						
39	41917	23 Aug. 1973	7 093.597	0.070602	65.7212	60.701	94.86	5 232.113	0.2054	0.01728	0.00092	-0.00084	0.76	60	5.6	6 592.77
			3	11	17	2	1	3	12	151						
40*	41936	11 Sept. 1973	7 085.756	0.069660	65.7261	6.434	84.53	5 240.802	0.2197	-0.00333	-0.00125	—	0.71	35	5.6	6 592.16
			2	13	11	2	2	2	12	30						
41	41955	30 Sept. 1973	7 080.770	0.068793	65.7223	312.001	74.14	5 248.564	0.2159	0.00003	0.00109	—	0.59	54	5.6	6 591.80
			1	5	11	1	1	1	8	25						
42	41964	9 Oct. 1973	7 074.956	0.068265	65.7191	286.144	69.21	5 252.809	0.2008	0.00132	0.00060	—	0.70	53	5.9	6 591.98
			1	13	15	2	2	1	12	23						
43	41974	19 Oct. 1973	7 071.225	0.067798	65.7211	257.360	63.78	5 256.968	0.2354	-0.00040	0.00055	—	0.84	69	5.5	6 591.81
			1	13	16	2	2	2	13	31						
44	42001	15 Nov. 1973	7 058.489	0.066226	65.7215	179.355	48.99	5 271.206	0.2326	-0.00329	-0.00187	0.00068	0.80	87	5.4	6 591.03
			1	8	8	1	1	1	12	90						

TABLE 2 (cont.)

mjd	date	$a$	$e$	$i$	$\Omega$	$\omega$	$M_0$	$M_1$	$M_2$	$M_3$	$M_4$	$M_5$	$e$	$N$	$D$	$a(1-e)$
45	42018	2 Dec. 1973	7050.835	0.065291	65.7190	130.001	39.59	224.43	5279.793	0.2264	0.00044	0.00035	0.73	48	5.8	6590.48
			2	11	13	1	1	1	3	13	16	9	0.91	63	6.1	6589.78
46	42043	27 Dec. 1973	7040.453	0.064012	65.7172	57.114	25.80	238.19	5291.478	0.2505	0.00049	—	—	—	—	—
			2	12	16	2	1	1	2	15	18	—	0.85	58	6.0	6589.63
47	42065	18 Jan. 1974	7028.889	0.062494	65.7146	352.628	13.69	145.93	5304.544	0.3787	0.00117	—	—	—	—	—
			2	23	18	1	1	1	2	15	17	—	0.92	88	5.3	6588.77
48*	42086	8 Feb. 1974	7016.036	0.060898	65.7148	290.715	1.99	100.21	5319.130	0.3241	—	—	—	—	—	—
			1	23	7	1	1	1	1	3	24	—	0.82	98	7.2	6587.61
49	42095	17 Feb. 1974	7010.655	0.060343	65.7110	264.058	356.92	119.88	5325.256	0.3174	—	—	—	—	—	—
			1	10	16	1	1	1	1	2	8	—	0.66	72	7.3	6587.42
50	42111	5 Mar. 1974	7001.028	0.059078	65.7061	216.502	348.01	90.52	5336.245	0.3403	0.00176	—	—	—	—	—
			1	20	13	1	1	1	1	10	7	—	0.83	76	7.3	6586.95
51	42126	20 Mar. 1974	6991.123	0.057812	65.7104	171.708	339.60	299.38	5347.593	0.3449	0.01520	—	—	—	—	—
			3	24	16	2	1	1	3	11	9	5	0.53	50	5.6	6586.27
52	42141	4 Apr. 1974	6980.508	0.056477	65.7076	126.696	331.07	326.52	5359.797	0.4404	0.00702	—	—	—	—	—
			1	14	12	1	1	1	1	15	19	—	0.76	68	3.9	6586.26
53	42146	9 Apr. 1974	6976.805	0.055978	65.6995	111.635	328.25	136.37	5364.066	0.4192	0.00300	—	—	—	—	—
			2	29	14	2	2	2	2	26	68	—	0.55	81	5.9	6585.67
54	42156	19 Apr. 1974	6969.039	0.055010	65.7010	81.434	322.51	181.24	5373.037	0.5275	0.00427	—	—	—	—	—
			1	10	10	1	1	1	1	10	12	—	0.46	94	4.2	6585.50
55*	42164	27 Apr. 1974	6962.938	0.054206	65.7046	57.193	317.93	355.70	5380.101	0.3923	0.00628	—	—	—	—	—
			2	12	5	1	1	1	2	17	53	36	0.64	80	7.6	6584.58
56	42172	5 May 1974	6957.488	0.053598	65.7066	32.883	313.32	221.01	5386.426	0.4450	0.00260	—	—	—	—	—
			2	16	13	1	2	2	2	7	5	3	0.38	69	5.9	6584.39
57	42191	24 May 1974	6946.439	0.052120	65.7003	334.911	302.41	96.75	5399.284	0.2556	0.00693	—	—	—	—	—
			1	9	8	1	1	1	2	7	9	6	0.41	74	5.8	6583.69
58	42212	14 June 1974	6936.988	0.050902	65.7027	270.534	290.31	193.72	5410.325	0.2742	0.00380	—	—	—	—	—
			1	8	11	1	2	2	1	8	8	3	0.42	72	7.9	6583.57
59*	42219	21 June 1974	6933.951	0.050514	65.7026	249.010	286.24	278.81	5413.880	0.2412	0.00324	—	—	—	—	—
			1	6	4	1	1	1	<1	4	10	7	0.41	74	5.8	6583.69
60	42230	2 July 1974	6929.254	0.049887	65.6986	215.123	279.85	100.37	5419.387	0.2473	0.00233	—	—	—	—	—
			1	7	9	1	1	1	7	36	5	2	0.42	72	7.9	6583.57
61*	42246	18 July 1974	6921.579	0.048938	65.6994	165.679	270.62	127.26	5428.406	0.2159	0.0005	—	—	—	—	—
			2	9	8	1	2	2	2	7	6	3	0.60	100	7.6	6582.85
62*	42253	25 July 1974	6918.709	0.048559	65.7015	143.995	266.51	336.64	5431.784	0.2984	0.00094	—	—	—	—	—
			2	10	7	1	2	2	3	13	29	18	0.54	71	5.3	6582.74
63	42260	1 Aug. 1974	6915.862	0.048205	65.7007	122.281	262.48	211.17	5435.139	0.2123	0.00197	—	—	—	—	—
			1	9	10	1	2	2	1	10	10	—	0.51	90	5.9	6582.48
64	42268	9 Aug. 1974	6912.330	0.047758	65.6991	97.427	257.80	149.02	5439.307	0.2613	0.00119	—	—	—	—	—
			1	10	12	1	2	2	1	9	8	—	0.57	84	6.8	6582.21
65	42291	1 Sept. 1974	6900.678	0.046222	65.6971	25.716	244.50	120.10	5453.091	0.3615	0.00627	—	—	—	—	—
			1	7	8	1	1	1	1	5	4	2	0.30	58	7.6	6581.71
66	42307	17 Sept. 1974	6889.308	0.044810	65.7039	335.558	235.09	350.06	5466.600	0.5569	0.00092	—	—	—	—	—
			3	23	19	2	3	3	4	15	10	5	0.92	62	7.7	6580.60

TABLE 2 (cont.)

MJD	date	<i>a</i>	<i>e</i>	<i>i</i>	$\Omega$	$\omega$	$M_0$	$M_1$	$M_2$	$M_3$	$M_4$	$M_5$	<i>e</i>	<i>N</i>	<i>D</i>	<i>a</i> (1- <i>e</i> )	
67	42319	29 Sept. 1974	6879.090	0.043597	65.7000	297.741	143.89	5478.787	0.4759	0.00091	0.00133	0.00091	—	64	80	7.8	6579.18
68	42329	9 Oct. 1974	6870.166	0.042337	65.6962	266.068	263.28	5489.467	0.8731	0.03047	-0.00252	0.03047	-0.00127	58	77	6.6	6579.30
69	42344	24 Oct. 1974	6852.653	0.040101	65.6968	218.251	331.39	5510.530	0.5587	0.01989	0.00105	0.01989	-0.00071	55	59	7.6	6577.85
70	42362	11 Nov. 1974	6832.209	0.037369	65.6917	160.364	8.78	5535.287	0.8884	0.00419	—	0.00419	0.88	62	7.4	6576.90	
71	42377	26 Nov. 1974	6812.269	0.034751	65.6846	111.610	63.62	5559.612	0.8531	0.00095	-0.00075	0.00095	0.00008	65	87	7.8	6575.54
72	42390	9 Dec. 1974	6794.376	0.032383	65.6868	68.966	185.84	5581.593	0.8182	0.01348	-0.00044	0.01348	-0.00044	64	73	7.6	6574.35
73	42398	17 Dec. 1974	6783.746	0.030927	65.6860	42.538	188.82	5594.721	0.8522	0.02166	0.00152	0.02166	-0.00034	71	77	7.6	6573.95
74	42413	1 Jan. 1975	6762.753	0.028166	65.6774	352.557	76.27	5620.798	0.7019	-0.00369	-0.00010	-0.00369	—	75	58	7.8	6572.27
75	42424	12 Jan. 1975	6749.215	0.026282	65.6821	315.608	76.82	5637.722	0.7013	-0.00165	0.00509	-0.00165	0.00101	62	61	7.0	6571.83
76	42438	26 Jan. 1975	6731.372	0.023941	65.6737	268.185	327.55	5660.158	0.7093	-0.00185	0.00312	-0.00185	0.00021	50	63	7.0	6570.22
77	42448	5 Feb. 1975	6718.089	0.022146	65.6664	234.063	148.53	5676.956	0.9131	0.00111	0.00121	0.00111	—	83	83	7.5	6569.31
78	42457	14 Feb. 1975	6703.003	0.020218	65.6642	203.099	142.43	5696.137	1.1440	-0.01118	0.00020	-0.01118	0.00026	62	64	7.2	6567.48
79	42468	25 Feb. 1975	6684.753	0.017818	65.6683	164.939	332.70	5719.484	1.0889	-0.00727	-0.00310	-0.00727	0.00020	51	63	7.1	6565.64
80	42478	7 Mar. 1975	6667.741	0.015782	65.6710	129.942	33.31	5741.392	1.3256	-0.03073	-0.00987	-0.03073	0.00196	74	53	5.6	6562.51
81	42484	13 Mar. 1975	6653.966	0.014201	65.6572	108.775	330.37	5759.234	1.6950	-0.02065	0.00577	-0.02065	—	74	54	5.8	6559.47
82	42490	19 Mar. 1975	6637.953	0.012374	65.6612	87.431	28.11	5780.091	1.8347	0.03097	0.00126	0.03097	-0.00134	54	37	5.7	6555.81
83	42496	25 Mar. 1975	6619.997	0.010263	65.6585	65.896	218.07	5803.630	2.3484	0.03972	-0.00125	0.03972	0.00218	86	30	5.9	6552.06
84	42501	30 Mar. 1975	6596.460	0.008059	65.6467	47.769	108.59	5834.727	3.8942	0.05041	0.05033	0.05041	—	81	16	2.9	6543.30
85	42505	3 Apr. 1975	6563.488	0.005051	65.6493	33.056	104.89	5878.759	8.5625	1.14266	0.30084	1.14266	0.05230	71	39	2.5	6530.34

\* Hewitt camera observations are used in determining these orbits.



TABLE 4. THE 15 DAILY SETS OF ORBITAL PARAMETERS BEFORE DECAY, WITH STANDARD DEVIATIONS

MJD	date	$a$	$e$	$i$	$\Omega$	$\omega$	$M_0$	$M_1$	$M_2$	$M_3$	$M_4$	$\epsilon$	$N$	$D$	$a(1-e)$
A	42492	21 Mar. 1975	6632.096	0.011667	65.6593	80.283	116.02	76.23	5787.752	1.997		0.83	86	1.44	6554.72
B	42493	22 Mar. 1975	6629.271	0.011345	65.6586	76.697	115.26	106.00	5791.453	1.772		0.91	100	0.94	6554.06
C	42494	23 Mar. 1975	6626.661	0.011060	65.6567	73.106	114.47	139.32	5794.875	1.878	0.41	0.91	100	0.93	6553.37
D	42495	24 Mar. 1975	6623.514	0.010745	65.6560	69.508	113.65	176.42	5799.007	1.970	4	0.73	46	0.80	6552.34
E	42496	25 Mar. 1975	6619.992	0.010386	65.6562	65.909	112.66	217.94	5803.636	2.706		0.49	78	0.80	6551.24
F	42497	26 Mar. 1975	6616.291	0.009949	65.6559	62.300	112.31	263.78	5808.507	2.413		0.94	79	0.80	6550.47
G	42498	27 Mar. 1975	6612.384	0.009636	65.6550	58.679	111.14	315.27	5813.658	2.794		0.93	79	0.93	6548.67
H	42499	28 Mar. 1975	6607.772	0.009124	65.6559	55.054	110.45	11.82	5819.747	3.516		1.04	94	0.99	6547.48
I	42500	29 Mar. 1975	6602.256	0.008580	65.6558	51.424	109.60	75.35	5827.044	3.758		0.84	100	0.86	6545.61
J	42501	30 Mar. 1975	6596.466	0.008049	65.6563	47.773	109.26	145.87	5834.719	3.936		0.96	96	0.93	6543.37
K	42502	31 Mar. 1975	6590.346	0.007515	65.6563	44.118	107.91	225.29	5842.850	4.364	0.44	0.75	77	0.92	6540.82
L	42503	1 Apr. 1975	6583.083	0.006914	65.6532	40.450	107.00	313.05	5852.525	5.356	5	0.79	92	0.92	6537.57
M	42504	2 Apr. 1975	6574.476	0.006177	65.6555	36.759	106.11	51.41	5864.025	6.194	0.63	0.82	51	0.80	6533.87
N	42505	3 Apr. 1975	6563.409	0.005188	65.6542	33.060	106.10	161.83	5878.865	8.756	10	0.59	72	0.63	6529.36
O	42506	4 Apr. 1975	6546.778	0.003945	65.6518	29.325	103.13	292.99	5901.288	14.992	3.77	0.93	88	0.88	6520.95
											5		77		
											5		38		